Effects of Alcohol on the Spatial Representation in the Hippocampal Formation

Debanjan Chowdhury
Roll No: MS15004

A dissertation submitted for the partial fulfilment
of BS-MS dual degree in Science

Under the guidence of
Dr. Satyajit Jena

June 2020

Indian Institute of Science Education and Research Mohali
Sector - 81, SAS Nagar, Mohali 140306, Punjab, India

Certificate of Examination

This is to certify that the dissertation titled **Effects of alcohol on the spatial representation in the hippocampal formation** submitted by **Debanjan Chowdhury** (Reg. No. MS15004) for the partial fulfillment of BS-MS dual degree programme of the Institute, has been examined by the thesis committee duly appointed by the Institute. The committee finds the work done by the candidate satisfactory and recommends that the report be accepted.

Dr. P. Balanarayan Dr. Samarjit Bhattacharyya Dr. Satyajit Jena
(Supervisor)

Dated: 15.06.2020

Declaration

The work presented in this dissertation has been carried out by me under the guidance of Dr. Satyajit Jena at the Indian Institute of Science Education and Research Mohali. This work has not been submitted in part or in full for a degree, a diploma, or a fellowship to any other university or institute. Whenever contributions of others are involved, every effort is made to indicate this clearly, with due acknowledgement of collaborative research and discussions. This thesis is a bonafide record of original work done by me and all sources listed within have been detailed in the bibliography.

Debanjan Chowdhury
(Candidate)

Dated: June 15, 2020

In my capacity as the supervisor of the candidate s project work, I certify that the above statements by the candidate are true to the best of my knowledge.

Dr. Satyajit Jena
(Supervisor)

Acknowledgement

First and foremost, I would like to thank my thesis supervisor, Dr Satyajit Jena, without whose help and supervision, this thesis would never have been possible. The discussions that I had with him has enhanced my capabilities as a researcher. He has taught me the importance of tackling a problem from different perspectives and has ignited a great deal of curiosity within me to explore computational approaches for solving problems in neuroscience. I would like to express my profound gratitude to Professor Hannah Monyer for allowing me to work under her tutelage in her state of the art lab at DKFZ (German Research Cancer Centre), Heidelberg, Germany. Her kind and practical nature made me feel at home in her lab. She is a constant source of inspiration to me for her impeccable work ethics. I am indebted to her for allowing me to work on the in vivo electrophysiological data which I collected in her lab. I am grateful to Dr Magdalena I. Schlesiger and Dr Duncan MacLaren for the encouraging supervision and valuable guidance during the whole internship and for providing me with this opportunity to conduct novel research. I am thankful to Dr Magdalena I. Schlesiger for teaching me the basics of in vivo electrophysiology and for providing critical help in analyzing the raw signal and in improving the quality of recordings. I am especially grateful to Dr Duncan MacLaren for all his valuable inputs and help in writing and editing this thesis. His gentle, patient and encouraging nature inspired me to work at my optimum potential. The discussions that I had with him have enhanced my understanding of this field. I am also immensely thankful to the medicine doctoral student Beate Throm for her technical assistance and meaningful discussions. She helped me a lot to get adjusted to the new surroundings and taught me the way to efficiently carry out the electrophysiological recordings. My days in Prof. Monyer's lab with her as a part of a team were quite enjoyable. I am grateful to the PhD students Isabel Barriuso, Xu Huang, Ting-Yun Yen & Maryam Najafian Jazi and postdoctoral researcher Dr Olga Kornienko for their help and support. I am thankful to all the other lab members at the DKFZ lab for their

advice and fruitful discussions as well.

I would like to thank Dr Samarjit Bhattacharyya and Dr N.G.Prasad for teaching neuroscience and biostatistics as elective courses respectively. The work done in the present study has greatly benefitted from the lessons learnt in their courses. I am also thankful to Dr P. Balanarayan for being very supportive of my endeavours and to always lend a helping hand in times of crisis. I am immensely thankful to Dr Yoganarasimha Doreswamy at NBRC, Manesar, Haryana and Dr Sachin Deshmukh at IISc, Bangalore for allowing me to work under their guidance as a part of short research projects in the previous semesters. They introduced me to the field of spatial memory and navigation and thus played a critical role in developing my interest in this field.

Lab members in Dr Satyajit Jena's lab also provided me with a lot of help and support. I am especially grateful to my peers Saurabh Bedi, Deesha Divecha, Rutik Manikandhan, Sveekruth S. Pai and the PhD student Rohit Kumar for the engaging discussions and help when I was stuck. I would like to express my gratitude to Innovation in Science Pursuit for Inspired Research (INSPIRE) Scholarship of the Department of Science and Technology (DST) and IISER Mohali for allowing me to pursue my interests and for providing financial, infrastructural and educational support.

I am indebted to Debjit Ghosh, Nilangshu Bhattacharyya, Ishan Sarkar, Adarsh R, Nikhil Tanwar, Amit Suthar, Apoorv Gaurav, Anubhav Jindal, Vivek Jadhav, Satyam Prakash, Swastik PG, Paresh Nath Das and Gaurav Singh for their invaluable support and the countless meaningful discussions throughout the BS-MS Dual degree program at IISER. I had an enjoyable, informative, interesting and enriching experience because of them. I consider myself to be extremely lucky to be a part of IISER Mohali community and am grateful to have brilliant budding scientists as my batchmates.

I would like to thank my family members who were my pillars of support. I would especially like to express my gratitude to my father because of whom I got interested in neuroscience in the first place. The innumerable discussions that I had with him about the human brain etched a deep curiosity in me to explore the field of neuroscience in greater

detail. I am grateful to my mother for giving me the necessary pep talk when I felt low and for supporting my scientific pursuits. I am thankful to my brother and grandmother who always encouraged me in my scientific ventures and were a healthy influence on me. Finally, I dedicate this present work to my grandfather who is no longer with us but was a great supporter of all my endeavours.

Debanjan Chowdhury
MS15004
IISER Mohali

List of Figures

Contents

Abstract

Episodic memory plays a critical role in everyday life activities. Spatial memory, which can be a type of episodic memory is essential for navigating through an environment. Alcohol is one of the most common household beverages. Moreover, alcohol as a substance of abuse is a very active area of research. However, the effects of alcohol on the spatial memory have not been investigated adequately and hence the underlying effects are poorly understood. The aim of the present study was to investigate the effects of acute alcohol intoxication on the CA1 region in the hippocampus at the cellular and the network level with the help of in vivo electrophysiology in awake, freely behaving parvalbumin-cre mice. Further, it is known that the medial septum plays a critical role in pacing the hippocampal local field potential (LFP) theta. Therefore, this study also aimed to find if the rhythmic activation of the parvalbumin containing cells in the medial septum, via optogenetic stimulation could restore the function of the hippocampus under the influence of alcohol. It was found in the present study that acute alcohol intoxication at a dosage of 1.5 g/kg, administered intraperitoneally led to a reduction in the mean firing rates of non-spatial cells immediately after the injection. Interestingly, no significant change was seen in the mean firing rate and the information score of the place cells following acute alcohol intoxication and the location of the place fields also remained stable. No significant change was seen in the mean firing rate of interneurons as well. At the network level, a significant drop in the LFP theta frequency and power was seen immediately after injecting alcohol. The suppression in the LFP theta frequency persisted throughout the recording session in the alcohol injected mice. Further, the optogenetic stimulation of the parvalbumin containing cells in the medial septum in the alcohol session did not reliably pace the hippocampal LFP theta since the LFP theta frequency dropped even while the stimulation was being done. Therefore, results from the present study provide evidence that acute alcohol intoxication causes changes in both cellular and network level in the CA1 region of the hippocampus of mice. Hence, a more

detailed research project with a goal to find the underlying mechanisms involved in causing the deficits in the spatial memory due to alcohol intoxication should be undertaken.

Chapter 1

Introduction

1.1 Scientific Bckground

Memory is a critical requirement for survival. From tiny unicellular organisms like E.coli and amoebae to complex multicellular organisms like rodents, dogs and humans, all living organisms employ different mechanisms to form memories which enable them to successfully interact with their environment (*1–4*). The process of forming a memory involves encoding, storing, retaining and subsequently recalling information and past experiences. Memory is primarily classified into declarative and non-declarative memory (*5*) (Figure 1.1). As the name suggests, declarative memory can be declared or expressed and hence is also called explicit memory. Non-declarative memory, on the other hand cannot be explicitly expressed and correspondingly is called implicit memory. Procedural memory, which stores information on how to do things is a type of non-declarative memory. Within declarative memory, there are two subclasses: semantic memory and episodic memory. Semantic memory processes ideas and concepts that are not drawn from personal experience. Episodic memory, on the other hand, is the unique memory of a specific event experienced by the subject. For instance, consider riding a bike. The mechanics of driving a bike is an example of procedural memory. However, the question about when did one first ride a bike or who invented the bike are examples of episodic and semantic memory respectively. ‘Mental time travel or the ability to mentally reconstruct personal events from the past is possible because of episodic memory which also helps in anticipating future events based upon these experiences (*5*, *6*).

Episodic memory is linked to the ability to state the important details of an event and the

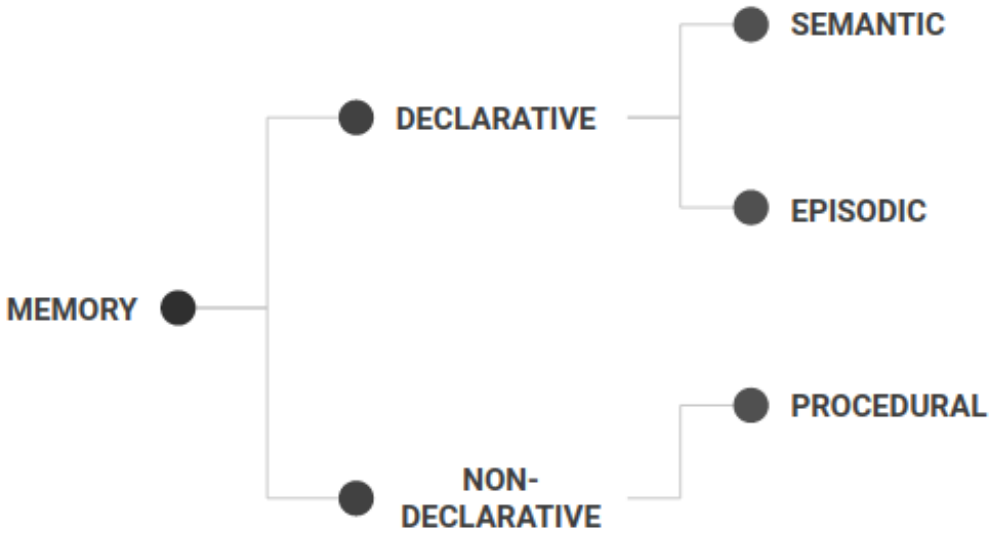

Figure 1.1: Classification of memory.

context in which it took place. However, for all animals except humans, the ability to declare is almost impossible to test. Correspondingly, it is hard to test if non-human animals have episodic memory. Moreover, many researchers question the ability of animals to 'mentally time travel' and relive an experience (*7*). To circumvent this problem, episodic memory tests are broken down into its fundamental components that the animal can answer, by focusing on the behavioural output. These components are what event took place, when did it happen and where did it take place (*8*). The researchers then design experiments that test these what-where-when components, which is also called episodic-like memory (*9*). In this context, random foraging tasks represent the simplest form of an episodic memory test. The food-deprived subjects move about in a box/maze (where), looking for food (what), when they are placed there, on the basis of previous experiences (when) (*10*, *11*). In such a task they have to learn to move about in the box/maze for food. These episodic-like tests could be more complex if more conditions are added, such as an odour task, where the animal receives the reward by entering the compartment in a maze (where) which has a particular odour (what) depending upon learned expectations (when) (*12*).

The most important structure for episodic and episodic-like memory is the medial temporal lobe. The study on this structure came to the limelight because of a patient named

Henry Molaison (H.M.). H.M. underwent bilateral medial temporal lobe resection as a cure for epilepsy. Interestingly, after the operation, he could no longer form new episodic memories (*13*, *14*). Medial temporal lobe consists of the hippocampal formation (HF) and the adjacent perirhinal, entorhinal and parahippocampal/postrhinal (in humans and rodents respectively) cortices also called extra hippocampal cortices (EHC) (*15*) (Figure 1.2). Bi-directional projections exist between the HF and the associated cortices which play a critical role for encoding, consolidation and retrieval of episodic memories (*16*, *17*). The HF consists of the dentate gyrus, hippocampus proper and the subiculum complex (prosubiculum, presubiculum, postsubiculum and parasubiculum; (*18*)). The hippocampus proper consists of three Cornu Ammonis (CA) subfields namely CA1, CA2 and CA3. The entorhinal cortices (EC; with medial: MEC and lateral: LEC subdivisions) receive projections from the parahippocampal/postrhinal and perirhinal cortices which themselves receive inputs from neocortical areas responsible for processing sensory information (*19*, *20*). This information is then relayed onto the hippocampus (*21*, *22*). It should be noted that reciprocal projections from the hippocampus to the EC also exist (*16*, *17*). Thus, there is extensive inter-connectivity between the HF and EHC which is important for its functioning. Similarly, the neocortex-hippocampus-neocortex circuit is also believed to play a crucial role in memory. Information flow in this circuit is strongly influenced by the relatively sparse projections from the subcortical structures, such as the septum (*23*).

The 'where' component of the episodic-like memory pertains to the question of the location of the event. This kind of memory is referred to as spatial memory. It is responsible for the recording of one's environment and spatial orientation. Spatial memory enables one to remember where a structure is in context to some other structure and thus helps in navigating through a place. Spatial navigation is thus tightly linked to the concept of spatial memory. Spatial navigation relies on the use of specific landmarks (spatial cues) as well as contextual information of the space (such as objects, shape, texture, odours, etc.) (*24*, *25*).

As a subset of episodic memory, the spatial memory is dependent upon the HF and EHC (*17*). Due to rapid progress in the field of the in vivo electrophysiological recordings in behaving rodents, the current understanding of how different cell types in this system interact to form spatial memories has increased exponentially. In this type of recordings, electrodes are used to measure the extracellular electrical activity which is also known as the local field

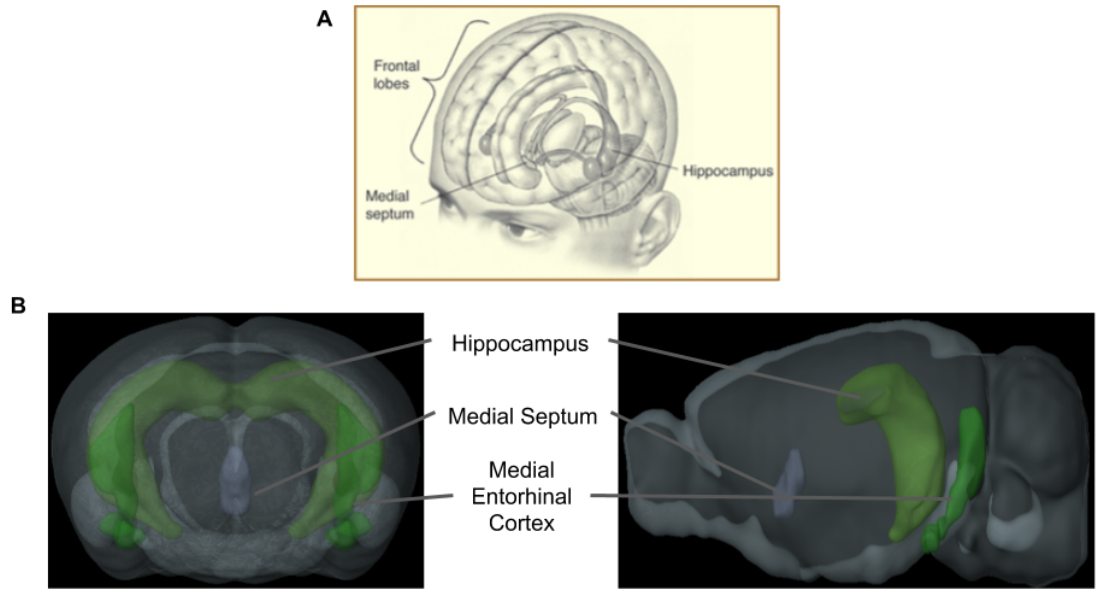

Figure 1.2: Hippocampus and medial septum in the human brain (A) and mouse brain (B) respectively. For B, the left figure shows the mouse brain coronally caudally (back) to rostrally (front) while the right figure shows the brain sagittally. A. Image source: MIT OCW, Clinical Psychology by David Lewis.; B. Images created using Allen Brain Atlas Application.

potential (LFP) of a brain region while the animal is freely moving in the environment (*26*) (Figure 1.3 A, B). This allows for a link between the electrophysiological activity at the neuronal level with the ongoing behaviour. Tetrodes which are essentially 4 electrodes intertwined together are used for these recordings to record the electrical activity from a very small cross-section. They serve the purpose of attributing the detected spikes to individual neurons, based on the relative amplitude of the spike signal received by the four-electrode wires (Figure 1.3 C, D). This enables the researchers to investigate the firing activity of the individual neurons while the animal performs a behavioural task (Figure 1.3 E). Upon using these tetrode recordings in the HF-EHC region, a diverse variety of cell types associated with distinct spatial memory representations have been characterized. Place cells which are pyramidal neurons present in the CA region of the hippocampus were the first spatially selective cells to be discovered (*27*) (Figure 1.3 F). These cells fire whenever the animal is in a particular location in the environment. The resulting spatially receptive field is called the place field. Subsequently, it was found that MEC also contains a variety of spatially selective cells such as grid cells (*28*), head-direction cells (*29*) and border cells (*30*) (Figure 1.3 F). Grid cells have multiple firing fields separated by an even spacing, forming a

grid-like map which is characterized by the periodic presence of equilateral triangle units (*28*). Head direction cells fire whenever the animal is looking in a particular direction and was first discovered in the dorsal pre-subiculum (*31*). These kinds of cells are also found in retrosplenial cortex (*32*), and subcortical regions like the thalamus (*33*). Finally border cells fire near the boundaries of the recording area (*30*). These cells are also present in the hippocampus, a subset of the place cells firing at the borders (*34*), and in the subiculum as well (*35*).

Interestingly, changes in the context or in the spatial cues of the environment can cause changes in the firing of spatially-selective cells. For instance, there may be changes in the firing properties of place cells in response to the experience of a new environment or the same environment in a new context (*36*). More specifically, the place cells may change their firing fields (that is, location) and/or their firing rates. The former is known as global remapping and the latter rate remapping (*37*).

The extracellular activity which is also called the Local Field Potential (LFP) sheds insight on the cooperative behaviour of the neurons (*26*). Theta rhythm (6-12 Hz) in the LFP is of particular interest with regards to memory. It is observed that place cells fire at progressively earlier phases of the theta rhythm. This phenomenon is called theta phase precession (*38*, *39*). Theta phase precession is thought to play an important role in episodic memory in terms of phase coding, enabling synaptic plasticity and/or sequence retrieval and prediction (*40*). The theta rhythm is thought to originate from the medial septum (MS) (*41*). The MS is predominantly composed of cholinergic, GABAergic and glutamatergic neurons (*42*). GABA or gamma-Aminobutyric acid, is the chief inhibitory neurotransmitter in the central nervous system (CNS) (*43*). The GABA containing afferents from the septum control the inhibitory interneurons in the hippocampus which in turn play an important role in coordinating the behaviour of a large number of pyramidal neurons in the hippocampus (*23*). Thus, GABA containing neurons in the medial septum are thought to be the key players in pacing the hippocampal LFP theta and consequently, the MS is also sometimes called the ‘pacemaker (*44*). A subset of the GABAergic neurons in the MS contain parvalbumin (PV), a calcium-binding protein (*45*). These PV containing GABAergic neurons have been proposed to be the key players in the pacemaker circuit in the MS (*44*). Therefore by extension, the MS is believed to regulate the hippocampal spatial representation since the LFP theta is critical for episodic memory (*46*). In fact, a recent study shows that the place cell

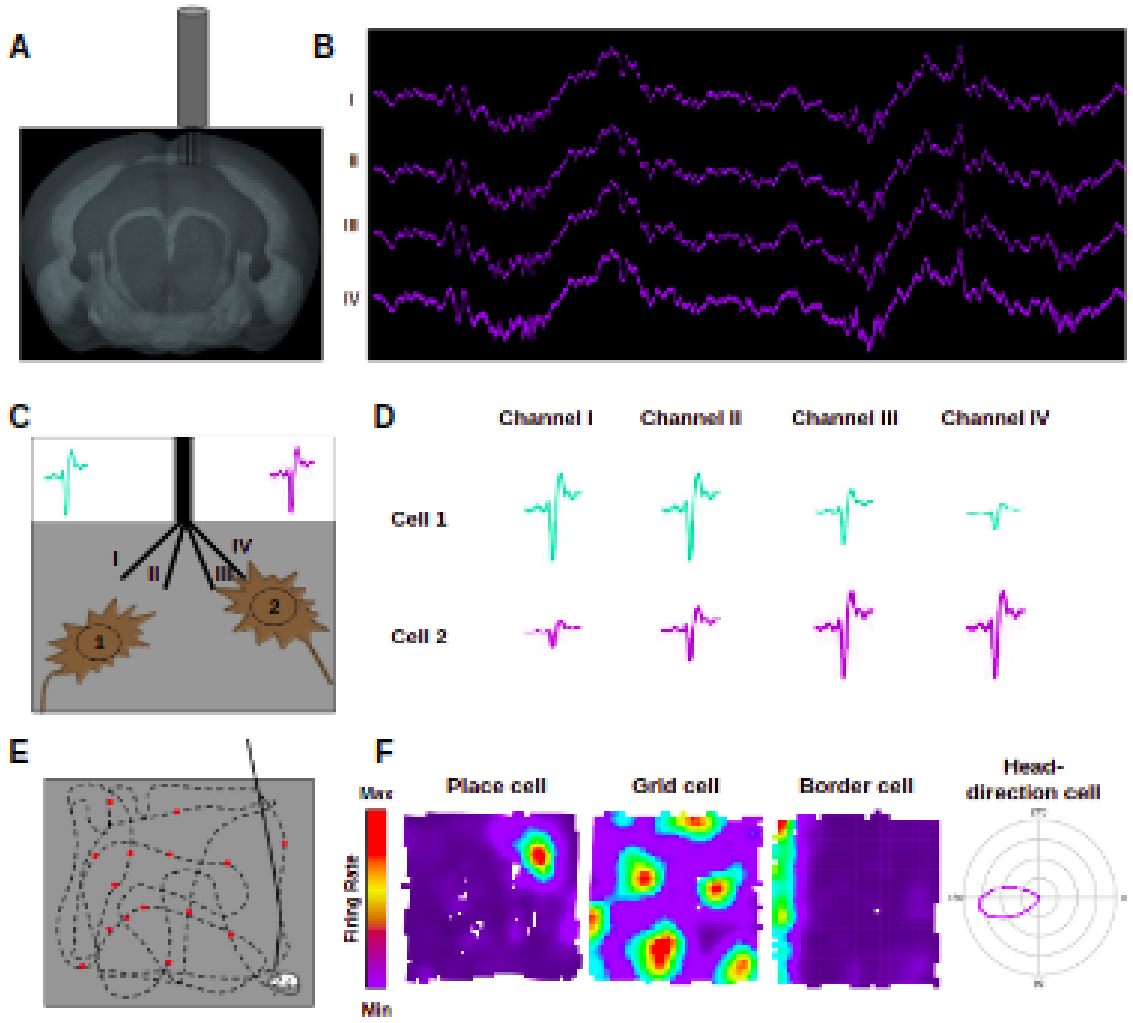

Figure 1.3: ***In vivo*** **electrophysiological recordings. A.** Multiple movable tetrodes (black lines) constructed of four intertwined electrodes each of which are placed inside a microdrive (grey cylinder) and implanted into the cortex. For CA1 recording, they are gradually lowered until a characteristic CA1 signal is seen. **B.** A characteristic example of raw recording traces (1s) obtained on each of the four wires. Each of these wires transmits the extracellular electric potential surrounding it, and the recorded signal is characterized by pronounced oscillatory activity at 6-12 Hz (theta oscillations) along with sudden bursts of synchronous fast field oscillations (140-200 Hz) called sharp-wave ripples. The action potentials are also picked up by these tetrodes. **C. & D.** Schematic demonstrating the concept of assigning spikes to individual single units. **C.** The placement of tetrodes in the layer of interest. Each of the 4 wires of a tetrode (I-IV) are in close vicinity of the 2 neurons (1-2) and thus collect the extracellular action potential signals. **D.** The extracellular action potential of the two neurons as experienced by each of the 4 wires of the tetrodes. The amplitude of the action potential changes according to the distance of the neurons from the wire (the greater the distance, the smaller the amplitude recorded). Thus, spikes can be sorted into separate clusters or single units, based on the amplitude of extracellular spike waveform experienced by the various wires of a tetrode. **E.** In random foraging tasks, animals are allowed to freely explore an open field environment (grey box) while action potentials (red spots) and position is simultaneously (black dashed line) recorded. **F.** The environment is divided into pixels and the average firing rate of each cell is color coded. The firing rate maps of a place cell from CA1, grid cell, border cell and head direction cell from MEC are shown.

firing alone cannot achieve spatial navigation without intact septal circuits (*47*).

Due to rapid advances in optogenetics, that is, the use of optics and genetics simultaneously, it is now possible to selectively activate subsets of neuronal populations and control them temporally via the use of lasers. In this technique, neurons are first genetically engineered to express light-sensitive proteins (opsins). Upon illuminating these neurons with the light of the matching frequency, the signalling pathways are correspondingly modulated depending upon the nature of opsin (*48*). For instance, Channelrhodopsin2 (ChR2) are light-gated cation channels which when illuminated with blue light, causes opening of channels, allowing passage of cations and leading to subsequent depolarizations (*49*). This pertains to the use of light to activate certain neuronal populations. However, to ensure only certain neuronal populations are targeted, transgenic mouse models having Cre-lox systems are used. For instance, for targeting the PV neurons, PV-cre transgenic mice are used (*50*). The success of the cre-lox system is attributed to the loxP sequences that are created de novo and the presence of cre-recombinase enzyme both of which are not present naturally in mammal systems. Typically a virus is used to infect the neuronal population of interest. The virus enters the cells (all cells at the site of injection) and causes them to express the genetic sequence encoded in the virus. For example, to activate ChR2 within PV-cre mice, viral vectors such as the adeno-associated viral (AAV) vector containing ChR2-mCherry flanked by a pair of canonical loxP sites is injected (*51*) (mcherry is a fluorescent protein which is used to tag components in a cell, in this case, the ChR2 protein so that they can later be visualized with fluorescence spectroscopy (*52*).). The cre transgenic rodent models contain the cre-recombinase enzyme in specific neuronal populations, PV+ cells in the example discussed. A genetically modified light-sensitive gene such as ChR2-mCherry is injected into a population containing the neuronal population of interest. As mentioned, the gene of interest is translated in all the cells producing ChR2-mCherry in the inverted (backwards) direction with loxP sites flanking this inverted region. Now, the cre-recombinase enzyme 'scans' through the sequence and identifies the loxP sites present at both the ends of the gene of interest as an instruction to invert the sequence between these sites. Therefore, the system causes only the cre positive cells (PV+ cells, in this case) to express the ChR2-mCherry in the forward (useful) direction. This functionally active ChR2 (gets attached to the neuronal membranes) can then be controlled by shining light of the corresponding frequency. Thus, advances in optogenetics have enabled researchers to ask targeted ques-

tions and consequently better understand the underlying network dynamics of neuronal populations. For instance, a recent study showed that medial septal GABAergic neurons can control the hippocampal LFP frequency outside of the endogenous theta range using optogenetic stimulation (*53*).

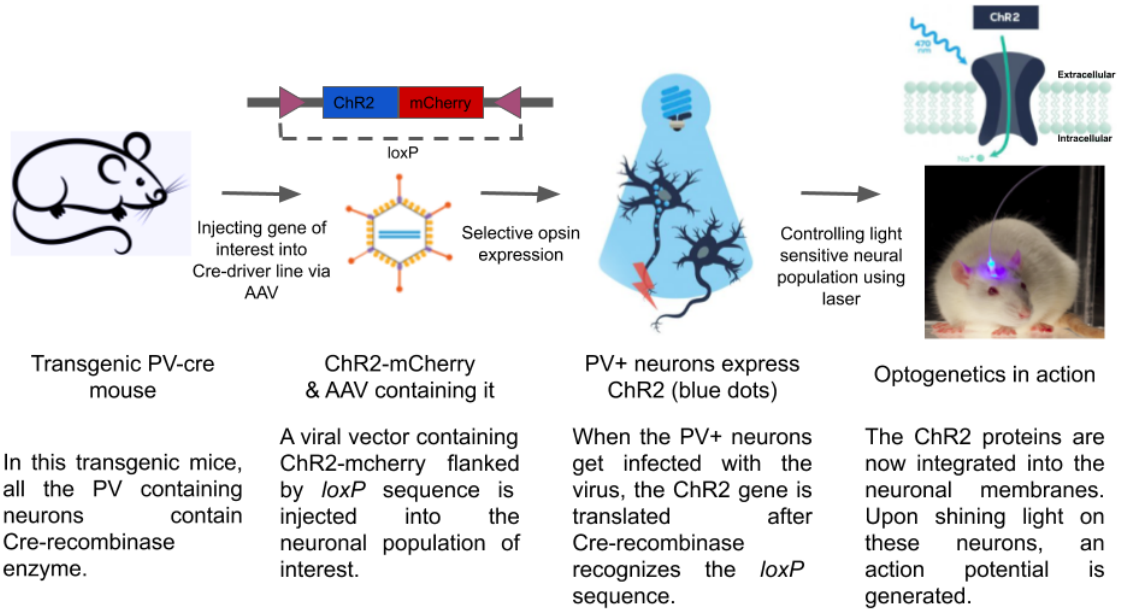

Figure 1.4: Schematic of methods used in optogenetics. The present schematic shows how ChR2 is specifically expressed in PV neurons in PV-cre transgenic mice and the neurons activated by a laser. The neuron and the ChR2 membrane proteins are adapted from the Neuroscience book (*48*). The mouse showing optogenetic response is taken from John B. Carnett / Getty Images. PV: Parvalbumin; ChR2: Channelrhodopsin 2; AAV: Adeno Associated Virus

How various substances such as drugs affect the memory systems has been studied quite extensively (*54–56*). Alcohol is one of the most abused substances worldwide (*57*). Studies have investigated the various aspects of alcohol usage such as feelings of pleasure, reward, relaxation and addiction (*58–60*). The question of the detrimental effects of alcohol in humans such as Korsakoff s syndrome (*61*) and memory blackouts (*62*, *63*) have been studied. However, there are very limited studies which investigate the effects of alcohol on the episodic memory. Therefore, the underlying reasons for the associated deficits in episodic memory is not well understood. The acute alcohol intake leading to the changes in the memory system at the molecular and biochemical levels (*64–66*) and at the behaviour level (*67–69*) in rodent models have been studied. However, in vivo electrophysiological studies dealing with recordings in the hippocampus investigating the effects of alcohol on spatial

memory is sparse (*70–72*). Research along these lines would help in enhancing insights about the effect of alcohol on spatial memory and also its effect on the cellular and network level. It is known that alcohol leads to a reduction in hippocampal theta activity (*73*, *74*). Further, this reduction in the LFP theta due to alcohol administration has been attributed to the MS (*75*). These findings raise the interesting possibility of reversing the damaging effects of alcohol on spatial memory by artificially activating the septum.

1.2 Hypothesis & Experimental Aims

It is a well-established fact that alcohol acts as a CNS depressant (*76*). A few previous studies suggest a reduction in the firing rate of the place cells after injecting alcohol (*72*) or a decrease in their spatial selectivity (*71*, *72*). However, they could not find any reduction in the firing rate of interneurons (*70*, *72*). It should be noted that these previous studies had very low number of interneurons to make claims. In fact, most of these previous studies had very low number of cells overall and hence their interpretations should be considered with caution. Therefore, there is still uncertainty about electrophysiological changes that occur after alcohol administration. Further, it has been proposed that the memory impairing effects of alcohol is due to the associated neurophysiological changes in the septohippocampal pathway (*75*).

This master thesis project aimed to look at the effects of alcohol on the CA1 region of the hippocampus. Specifically, the effects of alcohol on the hippocampal cells (place cells, interneurons, etc.) and the LFP theta with the help of in vivo electrophysiological recordings were investigated. Further, since the MS plays an important role in pacing the LFP theta, this study also aimed to find if the rhythmic activation of PV+ neurons in the septum could restore the function of the hippocampus at both the cellular and network (LFP theta) level under the influence of alcohol.

Chapter 2

Experimental Methods

2.1 Subjects

All mouse experiments were performed according to the guidelines for laboratory animal welfare (Regierungspräsidium Karlsruhe). In the present study, 11 adult male PV-cre mice were used (*50*). All the mice were individually housed in Plexiglass home cages and kept on a 12-h light/dark cycle and maintained at 85-90% of their free-feeding weight with free access to water. All experiments were performed during the light phase under dim light conditions.

2.2 Virus Injection & Microdrive Implantation

Mice were anaesthetized with isoflurane. An adeno-associated viral (AAV) vector containing a double *loxP*-flanked (floxed) inverted open (DIO) reading frame coding for ChR2-mCherry (AAV DIO *ChR2-mCherry*) (obtained from K. Deisseroth, Stanford University) was injected into the MS (which gets expressed in the presence of Cre recombinase) (*51*). The optic fibre (obtained from Thor Labs CFML21U , `https://www.thorlabs.com/newgrouppage9.cfm?objectgroup_id=6742`) was implanted 0.2 mm above the MS (Figure 2.1). The dura mater above the hippocampus (2.0 mm posterior and 1.7 mm lateral to bregma) was removed and a microdrive containing 4 independently movable tetrodes (constructed from $12\,\mu\mathrm{m}$-diameter tungsten wires (H-Formvar insulation with Butyral bond coat; California Fine Wire, Grover Beach, CA)) was implanted above the CA1 region. Two stainless steel screws above the cerebellum served as reference and ground

signals.

2.3 In vivo Electrophysiological Recordings

After a recovery period of one week, mice were restricted to 2-3 g of lab chow and trained in three 20-minute trials of random foraging in a black, square chamber (70x70x30 cm). The trials were separated by 10 minutes of rest in a 25x25x30 cm box. Exploratory behaviour was encouraged with sugar sprinkles (TestDiet, St.Louis, MO, USA) which were automatically dispensed from the ceiling in intervals of 20-25s.

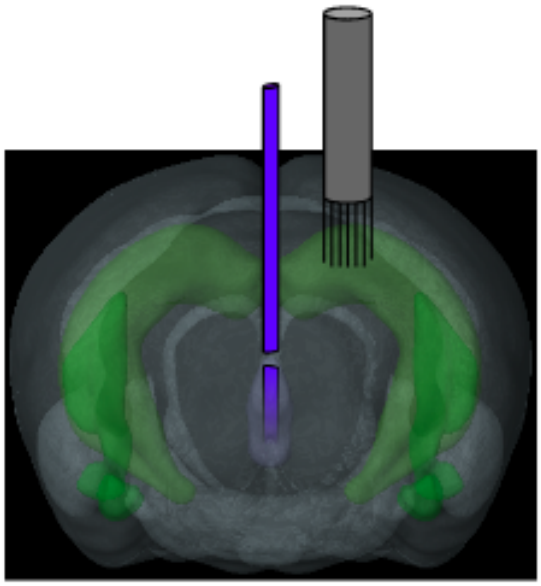

Figure 2.1: Schematic showing tetrodes in CA1 and optic fibre in the MS. The microdrive (grey cylinder) containing the tetrodes which are represented by black wires were lowered into the CA1 region of the hippocampus. The light green structure represents the hippocampus. PV+ cells in the medial septum (light blue structure) were activated by the laser stimulation of the implanted optic fibre represented by blue cylinder).

The tetrodes were lowered into the CA1 region daily by up to $\sim 100\,\mu\mathrm{m}$ (Figure 2.1). Tetrodes were considered to be located in the CA1 pyramidal cell layer if ripples (125-200 Hz) were observed during immobility and sleep. The signal was then recorded in the behavioural paradigm described below. Brain signals were recorded using RHD2000 (Intan Technologies) data acquisition systems and signals were sampled at 20kHz. For simultaneous position tracking, the signal of three LEDs attached to the headstage was recorded with a video camera. During the third open trial of a recording session, the implanted optic fibre (multimode IRVIS fibre, numerical aperture (NA) = 0.22) was connected to a diode-

pumped solid-state 473-nm laser (maximum, 50 mW; CrystaLaser) and laser pulses of 5 ms (2.5 mW) were delivered within the theta frequency range (6-12 Hz, the frequency was fixed at the start of the session). Once a pair of good recordings were obtained from one set of cells, tetrodes were lowered by $\sim 50\,\mu\mathrm{m}$ to obtain new cells and a new set of experiments was started.

2.4 Behavioural Paradigm

Each recording session consisted of four trials, starting with open foraging and alternating between rest and foraging trials. The foraging trials took place in the open field where mice received sugar sprinkles randomly as a reward for their exploratory behaviour. During rest trials, the mouse was placed in a rest box and did not receive sugar sprinkle reward. The recording protocol schematic is described in Figure 2.2. The first and the last open field represent baseline and recovery trials respectively. The mouse was administered saline or alcohol (1.5 g/kg) intraperitoneally and placed in the second open field session. The alcohol dosage used in the present study has been shown to cause spatial memory deficits (*72*, *77*). PV+ cells in the septum received stimulation in the third open field trial. Saline and alcohol recording sessions were performed in two consecutive days following which there was a gap of at least a day to ensure that the effects of alcohol had worn off.

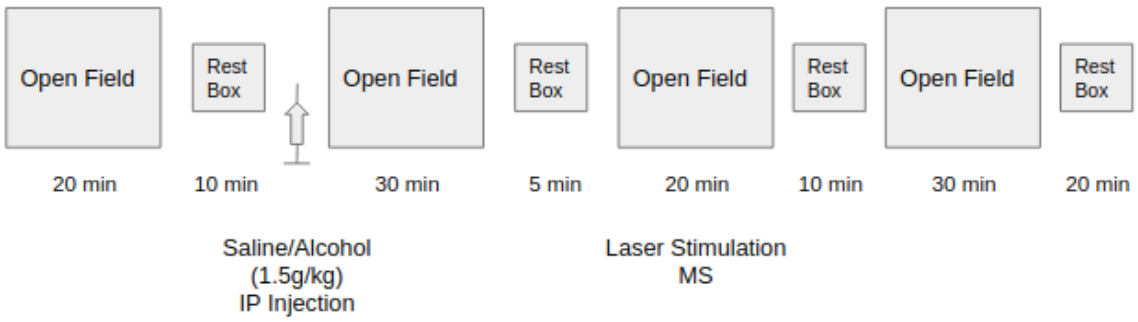

Figure 2.2: Schematic of the recording protocol. The mouse received intraperitoneal saline or alcohol injection just before the second open field trial. The PV+ cells in septum were stimulated in the third open field trial.

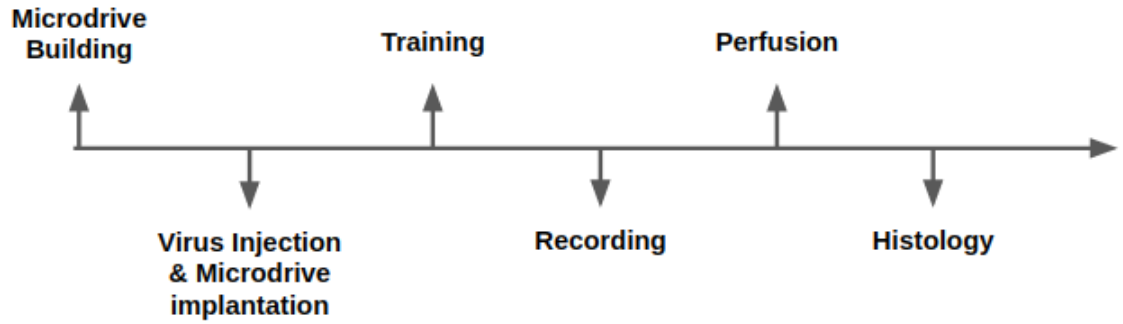

Figure 2.3: Summary of the Workflow. The workflow involved *in vivo* electrophysiology recordings.

2.5 Histology

After experiments were finished, mice were transcardially perfused with phosphate saline buffer (PBS) followed by 4% paraformaldehyde (PFA) solution. Fifty-micron sections through the region covering the MS were cut coronally on a vibratome and stained with DAPI for visualization of virus and optic fibre tract. The region covering the dorsal hippocampus was cut sagittally and stained with cresyl violet for observation of tetrode tracts.

2.6 Analysis of Electrophysiological Data

2.6.1 Inclusion Criteria

For addressing the effect of acute alcohol intoxication on the hippocampus, all the mice which had their tetrodes in the CA1 region represented by sharp-wave ripples and later verified by histology were used. If the mice did not show any units, but histology showed the presence of tetrodes in the CA1 region, then these sessions were considered for LFP analysis in addition to those which had units. For LFP analysis, only paired sessions were used. So these sessions/units were used for the first two open field trial analysis.

In order to tackle the question of the effect of stimulation of PV+ cells in the MS on the hippocampus and the recovery of units/LFP theta in the alcohol sessions, only those mice which showed a laser response were considered for analysis. Therefore, this subset of sessions/units was used for the third and the fourth open field trial analysis.

2.6.2 Unit Classification and Analysis of Single Cell Data

For each session, spikes were extracted off-line with custom-written software and assigned to individual single-units using Klustakwik (`http://klustakwik.sourceforge.net/`), followed by manual refinement with Klusters. Single units were then classified on the basis of the mean firing rate by creating firing rate maps. To create these rate maps, occupancy maps were first created by dividing the recording environment into 2x2-cm bins and computing the time spent in each bin followed by smoothing with a Gaussian kernel (s.d.=3cm). The number of spikes in each bin (the spike map) was then divided by the corresponding bin of the occupancy map. The resulting firing rate maps were smoothed with the Gaussian kernel (*78*). Putative excitatory cells were defined to have a mean firing rate (MFR) of $>$ 0.1 Hz and $\leq$ 10 Hz, while the putative interneurons (fast-spikers; FS) were defined to have a mean firing rate of $>$ 10 Hz. The excitatory cell group was further divided into spatial (place cells) and non-spatial cells based on the firing properties in the first open field exploration trial. The spatial information score used to quantify spatial selectivity of each cell was calculated as

$$I = \sum_{i=1}^{N} p_i \frac{\lambda_i}{\lambda} \log_2 \frac{\lambda_i}{\lambda} \tag{2.1}$$

where p_i is the occupancy probability of bin *i* in the firing map, λ_i is the firing rate in bin *i*, and λ is the mean firing rate of the neuron (*39*). Place cells were defined to have an information score $\geq$ 0.8.

The ratio of the MFR of different open field trials with respect to the first open field trial was computed for all the three cell types to determine if there was any difference in the alcohol sessions as compared to the saline sessions. To test whether the information score decreased upon alcohol exposure as compared to saline, the ratio of the respective open field trials with respect to the first open field trial were calculated.

2.6.3 Local Field Potential Analysis

For each tetrode, a time-frequency spectrogram from 0 to 16 Hz was calculated via the Chronux (`http://www.chronux.org/`) function mtspecgramc() using a window size and time step of 20 s and 10 s, respectively. The LFP theta frequency was taken as the frequency at maximum power within the 6-12 Hz frequency band of the time-averaged

spectrogram (*79*). The relative power was then taken as the maximum power of the normalized spectrum within the 6-12 Hz frequency band. The ratio of the respective open field trials with respect to the first open field trial was computed to find the difference in the theta frequency and relative power across alcohol sessions compared to saline sessions. The same parameters were calculated after applying a speed filter of 5 cm/s to check if the same relations held true when the mice were running.

2.6.4 Statistical Analysis

All statistical tests were two-sided with α = .05. Shapiro-Wilk test was performed to test for normality. In case of non-normal distribution, median statistics was performed and the data was represented in the form of boxplots with the box representing 25-75 percentile of the data (interquartile range; IQR), a horizontal black line within the box representing the median and the whiskers were represented as black vertical lines at 5 and 95 percentile values. Wilcoxon-rank sum test was used for between-group comparisons with the null hypothesis being the medians of both the groups were the same. Most of the comparisons were between saline and alcohol sessions as the two groups.

Chapter 3

Results

The result section has been divided into 4 major sections depending upon the open field trials. The first open field trial was termed Baseline trial since it was the same in terms of the experimental context for both saline and alcohol sessions. Saline or alcohol was injected intraperitoneally (i.p.) just before the start of the second open field trial. Therefore, this trial was termed Post Saline or Post Alcohol or collectively, Post Injection trials. The PV+ cells in the MS were stimulated in the third open field trial and thus the trial was correspondingly called Septum Stimulation trial. The final open field trial was called the Recovery trial since the effects of alcohol were expected to disappear by that time (Figure 3.1).

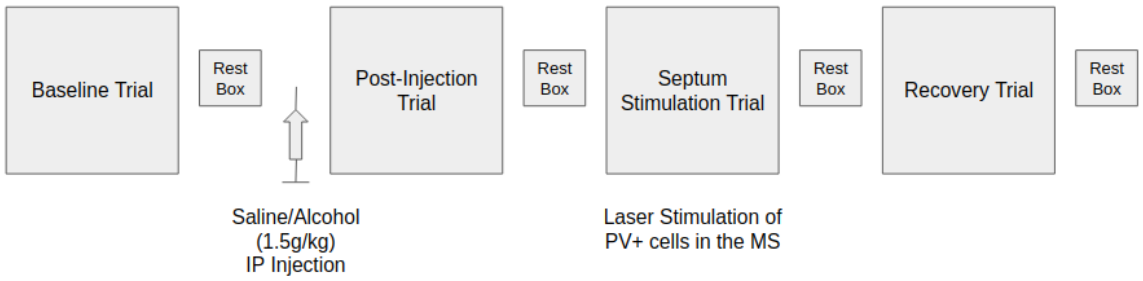

Figure 3.1: Schematic showing the four trials involved in both saline and alcohol sessions.

For each of these trials, mean firing rate (MFR) analysis, information score analysis and LFP theta frequency and relative power analyses were carried out. All of these measures were calculated as ratios with respect to the Baseline trial for the Post Injection, Septum Stimulation and Recovery trials.

For Baseline and Post Injection trials, 284 recording sessions from 11 mice were considered for the LFP analysis. For the effect of run on the LFP analysis, a subset of 240 sessions was

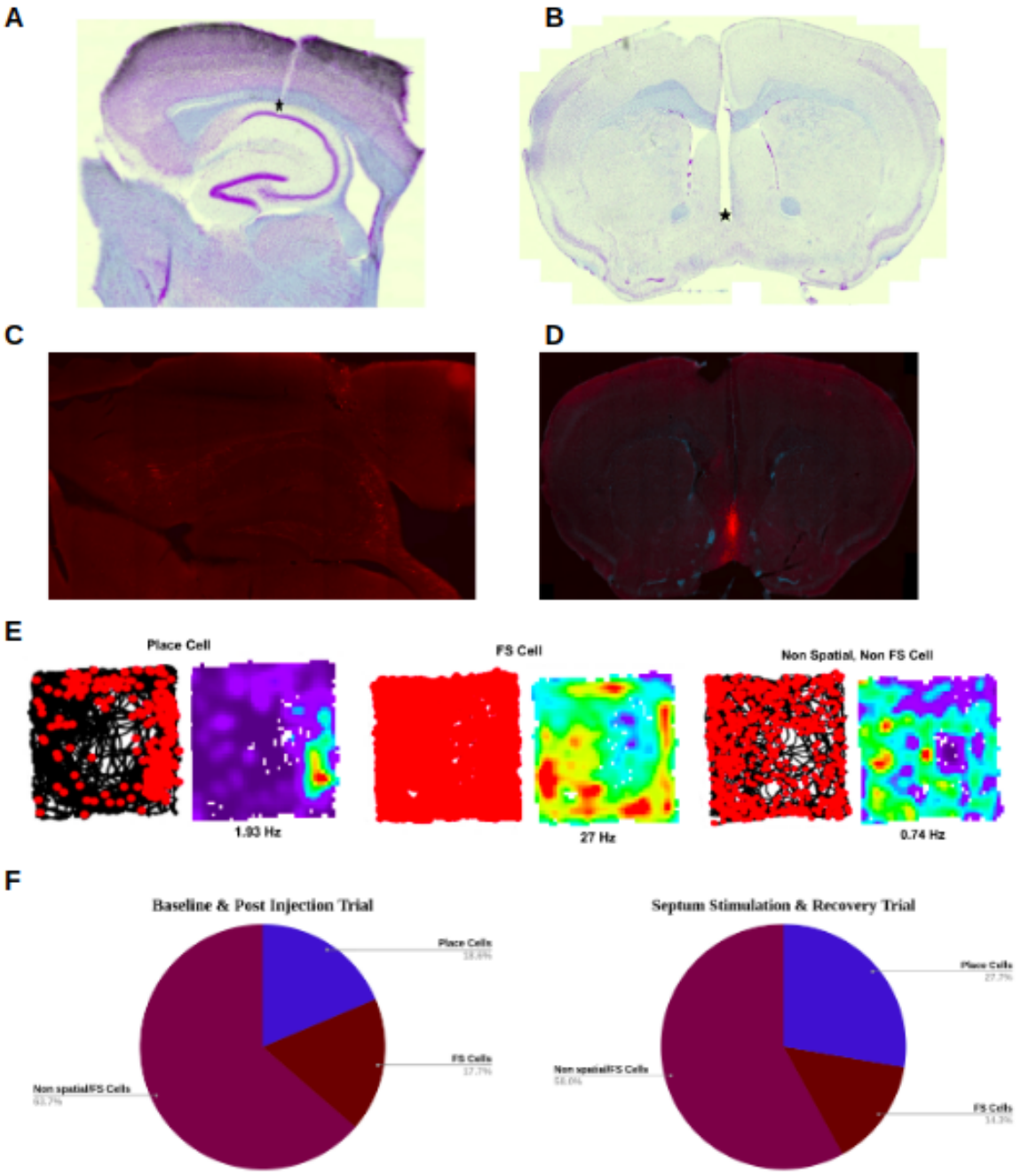

Figure 3.2: Representative examples from histology, cell types and summary of recording tetrodes. The Nissl stain shows the tetrode track in the CA1 region **A.** and the optic fibre track in the MS region **B.** visualized as a white vertical bar. The asterisk represents the recording position in the CA1 and the septal stimulation site at the MS. **C.** & **D.** Fluorescence images showing the virus spread in the mice brain slices. The fluorescent red dots (cell bodies) and branches (axons) in **C.** shows the expression of the virus in the CA region in the hippocampus. The red dots (cell bodies) in **D.** shows the expression of the virus in the MS region. **E.** Examples of different classes of neurons in the CA1 region are shown by their spike on path maps (where red dot denotes spikes and the black line represents the path traversed by the mice) and the firing rate maps. The frequency value at the bottom of the rate maps represents the mean firing rate. **F.** The pie charts show the distribution of the cell types recorded and analysed in baseline and post-injection trials (left) and in septum stimulation and recovery trials(right).

considered. A total of 531 single-units were recorded from 9 mice and were considered for the subsequent analysis. The two mice were excluded from the unit analysis since they did not yield any units. Out of these, 99 were place cells (18.6 %), 94 were fast-spiking (FS), that is, putative interneurons (17.8 %) and the rest 338 were non-spatial cells (63.4%) (Figure 3.2, F). The histology confirmed the presence of tetrodes in the CA1 region in these mice (Figure 3.2, A).

For Septum Stimulation and Recovery trials, 150 recording sessions from 7 mice were considered for the LFP analysis. The other 4 mice did not show any laser stimulation response. For the effect of run on the LFP analysis, a subset of 112 recording sessions was considered. A total of 231 single-units recorded from these 7 mice were considered for the unit analysis. Out of these, 64 (27.7%) were place cells, 33 (14.3%) were fast spikers and 134 (58.0%) were non-spatial, cells (Figure 3.2, F). The histology confirmed the presence of the optic fibre in the MS and the expression of the virus in these mice (Figure 3.2, B;C;D). In the four remaining mice, one of them had poor virus expression, while in two others the optic fibre was off to one side in the MS. For the fourth mice, probably the optic fibre got damaged during implantation since both the virus expression and fibre implantation site in the MS were correct.

3.1 Baseline Trial

3.1.1 Mean Firing Rate Analysis

The following analysis was carried out to examine if there was a significant difference in the MFR of the units between saline and alcohol sessions in the baseline trial. The median saline session MFR for 284 units was found to be 1.48 Hz, IQR = 0.56 - 6.82 Hz (Figure 3.3, A). The median alcohol session MFR for 247 units was found to be 1.92 Hz, IQR = 0.70 - 6.04 Hz (Figure 3.3, A). There was no significant difference in the baseline trial between saline session and alcohol session units (Wilcoxon rank-sum test: $p = 0.53$). Since potential effects could get masked if the different cell groups behave in opposite ways, the same analysis was computed for the individual subpopulations: place cells (saline(47): median = 0.53 Hz , IQR = 0.28 - 0.94 Hz; alcohol(52): median = 0.67 Hz, IQR = 0.30 - 1.17 Hz; Figure 3.3, B), FS (saline(53): median = 20.3 Hz, IQR = 15.69 - 28.04 Hz ; alcohol(41): median = 20.9 Hz, IQR = 15.69 - 28.23 Hz ; Figure 3.3, C) and non-spatial

cells (saline(184): median = 1.28 Hz, IQR = 0.57 - 3.63 Hz; alcohol(154): median = 2.00 Hz, IQR = 0.78 - 4.15 Hz; Figure 3.3, D). No significant difference was found in the MFR in any of the subpopulations between the two sessions (Wilcoxon rank-sum test, place cells: p = 0.44; FS cells: p = 0.98; non-spatial cells: p = 0.09). Thus, there was no difference in the MFR of the units between saline and alcohol sessions in the baseline trial.

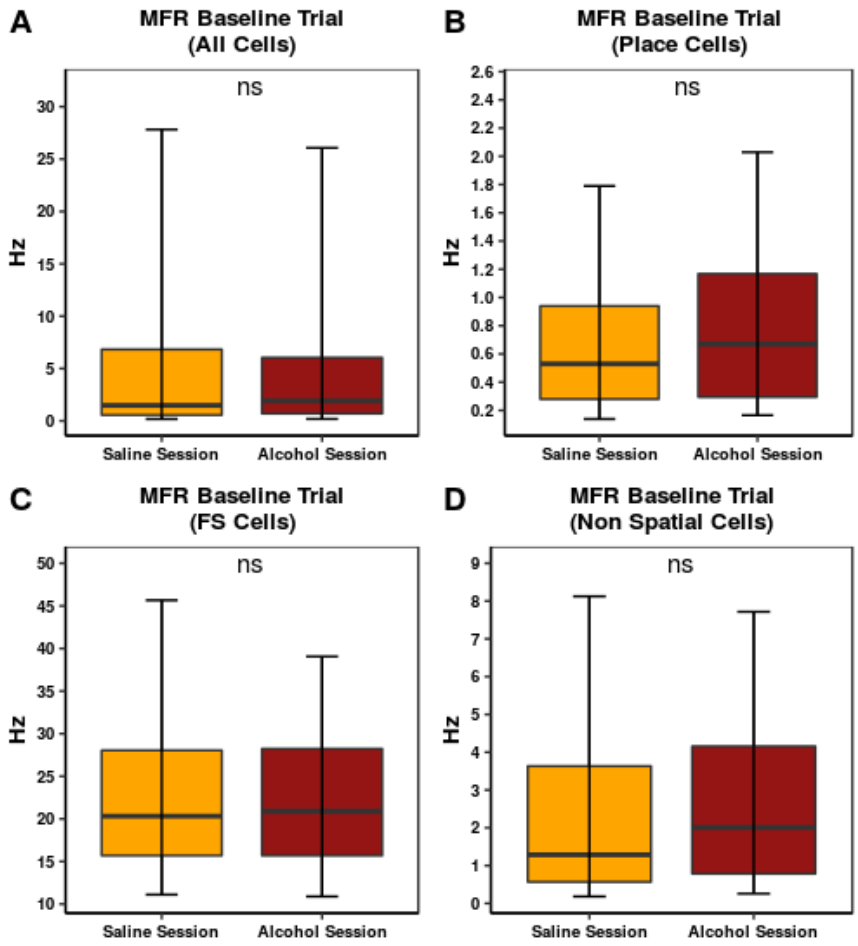

Figure 3.3: Boxplots representing the comparison of the baseline trial MFR scores between saline session and alcohol session units. **A.** MFR of all the units pooled together. **B.** MFR of place cells. **C.** MFR of fast-spikers. **D.** MFR of non-spatial cells. No significant difference was found between the MFR of saline session and alcohol session units in the baseline trial. The central bar represents the median, the whiskers represent the 5th and 95th percentile. ns: not significant.

3.1.2 Information Score Analysis

The following analysis was investigated to determine if there was a difference in the information score of place cells between saline and alcohol sessions before injecting saline or alcohol. The median information score for 47 place cells was found to be 1.22, IQR =

0.97 - 1.67 for the saline sessions (Figure 3.4). The median information score for 52 place cells was found to be 1.19, IQR = 0.92 - 1.68 for the alcohol sessions (Figure 3.4). There was no significant difference in the information score of the place cells in the baseline trial between saline session and alcohol session place cells (Wilcoxon rank-sum test: p = 0.65). Thus, the place cells had similar information scores in both saline and alcohol sessions in the baseline trial.

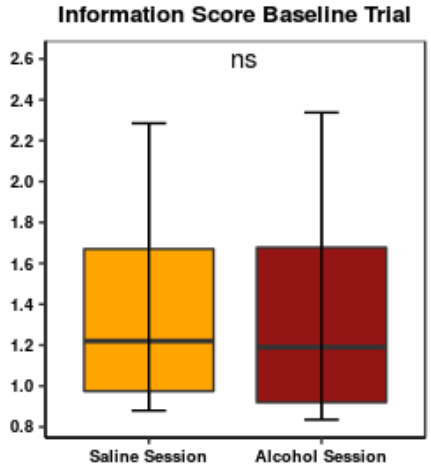

Figure 3.4: Boxplot representing the comparison of the baseline trial information scores of place cells between saline and alcohol sessions. No significant difference was found between the two sessions. The central bar represents the median, the whiskers represent the 5th and 95th percentile. ns: not significant.

3.1.3 LFP Theta Frequency

The LFP theta frequency for the baseline trial was computed to probe if the same theta rhythm frequency was present for both the saline and alcohol sessions before any interventions. The median LFP theta frequency in the baseline trial of 140 saline sessions was 8.19 Hz, IQR = 7.96 - 8.43 Hz (Figure 3.5, A). The median LFP theta frequency in the baseline trial of 140 alcohol sessions was 8.19 Hz, IQR = 7.98 - 8.37 Hz (Figure 3.5, A). There was no significant difference in the LFP theta frequency in the baseline trial for alcohol sessions as compared to the saline sessions (Wilcoxon rank-sum test, p = 0.96). Thus, the LFP theta frequency was similar in the baseline trial for both saline and alcohol sessions.

3.1.4 LFP Theta Power

The LFP theta power for the baseline trial was computed to examine if there was any difference in the theta power between the saline and alcohol sessions before any interventions.

The median LFP theta power in the baseline trial of 140 saline sessions was 5.99, IQR = 4.94 - 6.64 (Figure 3.5, B). The median LFP theta power in the baseline trial of 140 alcohol sessions was 5.71, IQR = 4.87 - 6.44 (Figure 3.5, B). There was no significant difference in the LFP theta power in the baseline trial for alcohol sessions as compared to the saline sessions (Wilcoxon rank-sum test, p = 0.17). Thus, the LFP theta power was similar in the baseline trial for both saline and alcohol sessions.

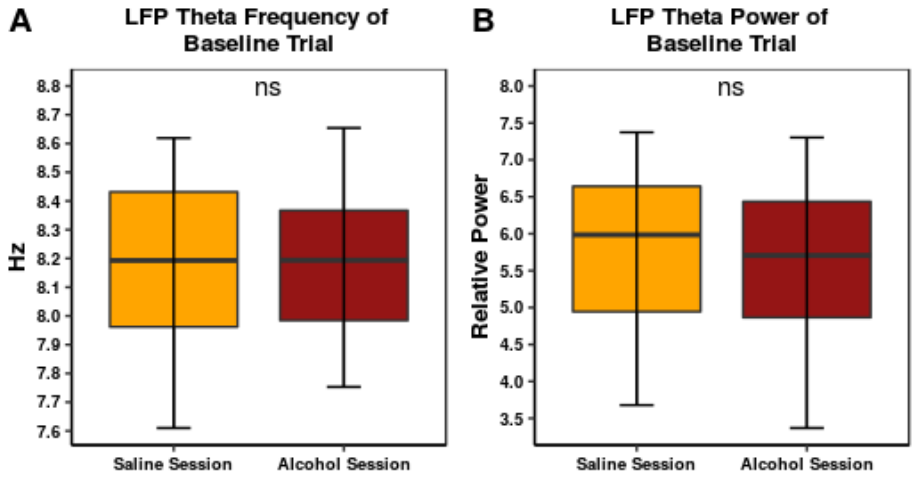

Figure 3.5: Boxplots representing the comparison of the baseline trial LFP theta frequency (A) and power (B) between saline and alcohol sessions. No significant difference was found between the saline and alcohol sessions for both theta frequency and power comparisons. The central bar represents the median, the whiskers represent the 5th and 95th percentile. ns: not significant.

3.1.5 Speed Filtered ($\geq$5 cm/s) LFP Theta Frequency

The following analysis was carried out to investigate the differences in the LFP theta frequency between saline and alcohol sessions when the mice were running in the baseline trial. The median LFP theta frequency in the baseline trial of 120 saline sessions was 8.20 Hz, IQR = 7.98 - 8.43 Hz (Figure 3.6, A) while the mice were running. The median LFP theta frequency in the baseline trial of 120 alcohol sessions was 8.21 Hz, IQR = 7.98 - 8.39 Hz (Figure 3.6, A) while the mice were running. There was no significant difference in the LFP theta frequency of the baseline alcohol sessions as compared to the baseline saline sessions (Wilcoxon rank-sum test, p = 0.95) when the mice were running. Thus, no significant difference was found in the LFP theta frequency between the saline and alcohol sessions in the baseline trial when the mice were running.

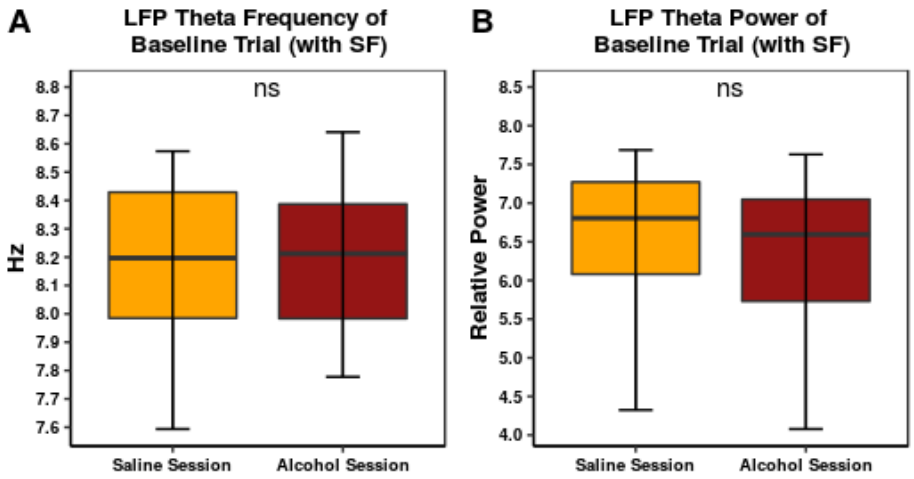

Figure 3.6: Boxplots representing the comparison of the baseline trial LFP theta frequency (A) and power (B) between saline and alcohol sessions when the mice were running (after applying a speed filter of 5 cm/s). No significant difference was found between the saline and alcohol sessions in both theta frequency and power comparisons. The central bar represents the median, the whiskers represent the 5th and 95th percentile. SF: Speed Filter ($\geq$5 cm/s); ns: not significant

3.1.6 Speed Filtered ($\geq$5 cm/s) LFP Theta Power

The LFP theta power for the baseline trial while the mice were running was investigated to ascertain if there was any difference in the same between saline and alcohol sessions. The median LFP theta power in the baseline trial of 120 saline sessions was 6.80, IQR = 6.08 - 7.27 (Figure 3.6, B) after applying a speed filter of 5 cm/s. The median LFP theta power in the baseline trial of 120 alcohol sessions was 6.60, IQR = 5.73 - 7.05 (Figure 3.6, B) after applying a speed filter of 5 cm/s. There was no significant difference in the LFP theta power in the baseline trial for the alcohol sessions as compared to the saline sessions when the mice were running (Wilcoxon rank-sum test, p = 0.08). Thus, no significant difference was present in the LFP theta power in the baseline trial while the mice were running between saline and alcohol sessions.

3.1.7 Within Trial Comparison With and Without Speed Filter

The following analysis was carried out to investigate if there was a difference in the LFP theta frequency and power within the baseline trial when the mice were running compared to the average movement of the mice throughout the trial. The median values for both the baseline theta frequency and the baseline relative theta power for both saline and alcohol

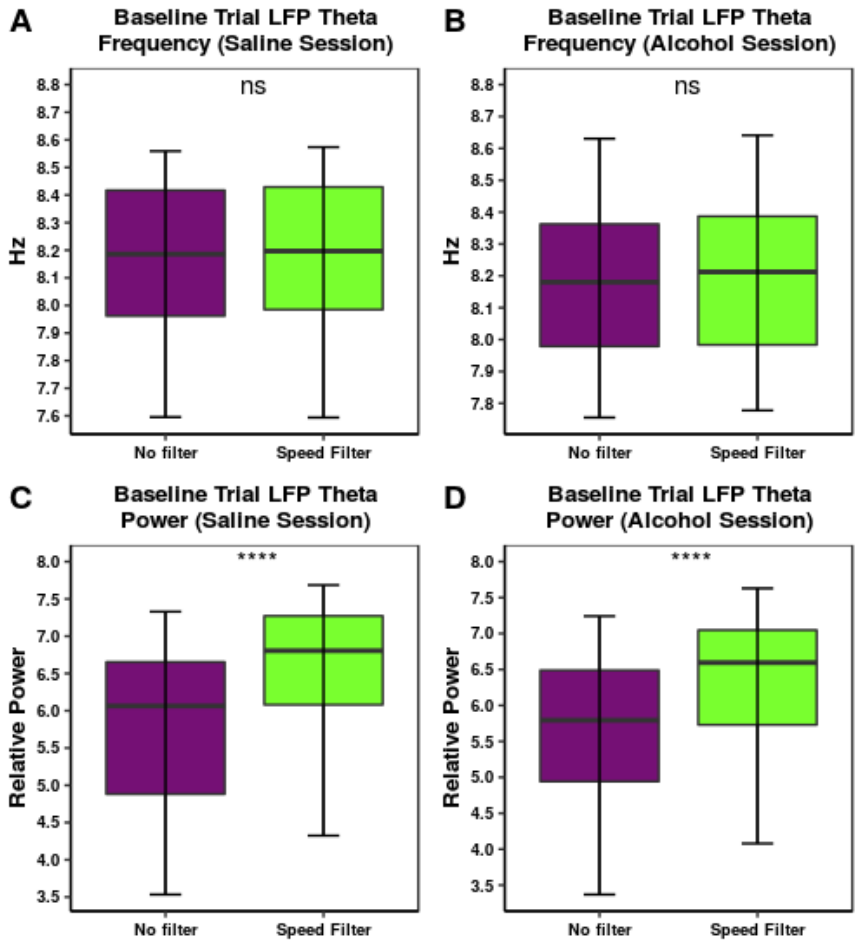

Figure 3.7: Boxplot representing the comparison of the no-speed filter and speed filter (5 cm/s) for the baseline trial while looking at LFP theta frequency (top) and relative power (bottom) in saline (left) and alcohol (right) sessions. No statistically significant difference was found in the LFP theta frequency when the mice were running compared to their average movement speed throughout the baseline trial in both saline **(A.)** and alcohol **(B.)** sessions. A significant increase in the relative LFP theta power was found when the mice were running in both saline **(C.)** and alcohol **(D.)** sessions. The central bar represents the median, the whiskers represent the 5th and 95th percentile.

sessions have already been given. Theta frequency was not found to be significantly different after application of speed filter compared to when there was no speed filter in both saline and alcohol sessions (Wilcoxon rank-sum test, Saline: p = 0.68, Figure 3.7, A; Alcohol: p = 0.53; Figure 3.7, B). Relative theta power, on the other hand, was found to be significantly greater when the mice were running (with speed filter) as compared to when there was no speed filter in both saline and alcohol sessions (Wilcoxon rank-sum test, Saline: p = 2.19e-8, Figure 3.7, C; Alcohol: p = 2.93e-7, Figure 3.7, D). Therefore, the LFP theta frequency did not change significantly when the mice were running compared to their average movement speed throughout the trial, whereas the LFP theta power significantly increased when the mice were running in both saline and alcohol sessions in the baseline trial.

3.2 Post-injection Trial

3.2.1 Mean Firing Rate Analysis

The following analysis was carried out to examine if there was a significant difference in the MFR of the units between saline (control) and alcohol sessions immediately following saline or alcohol injection. The median saline MFR ratio of the post-injection trial with respect to the baseline trial for 284 units was found to be 1.05, IQR = 0.79 - 1.46 (Figure 3.8, A). The median alcohol MFR ratio for 247 units was found to be 0.91, IQR = 0.67 - 1.33 (Figure 3.8, A). There was a significant difference in the MFR ratios between saline and alcohol group units (Wilcoxon rank-sum test: p = 0.01). Individual subpopulations were investigated to figure out the contributions of all these groups: place cells (saline(47): median = 1.08, IQR = 0.84 - 1.71; alcohol(52): median = 1.12, IQR = 0.84 - 1.66; Figure 3.8, B), fast spikers (saline(53): median = 0.85, IQR = 0.75 - 0.99; alcohol(41): median = 0.75, IQR = 0.66 - 0.93; Figure 3.8, C) and non-spatial cells (saline(184): median = 1.13, IQR = 0.84 - 1.62; alcohol(154): median = 0.92, IQR = 0.63 - 1.40; Figure 3.8, D). No significant reduction was found in the MFR ratios in case of place cells following alcohol administration (Wilcoxon rank-sum test, place cells: p = 0.76). A reduction in the MFR ratio was observed in FS following acute alcohol intoxication which was not statistically significant (Wilcoxon rank-sum test, FS cells: p = 0.07). However, a significant drop in the MFR ratio of non-spatial cells was observed following alcohol administration (Wilcoxon rank-sum test, non-spatial cells: p = 0.003). Therefore, a statistically significant reduction

in the MFR ratio (post-injection trial with respect to baseline trial) of non-spatial pyramidal neurons was observed immediately after i.p. injection of alcohol. The same trend was not observed for place cells and FS.

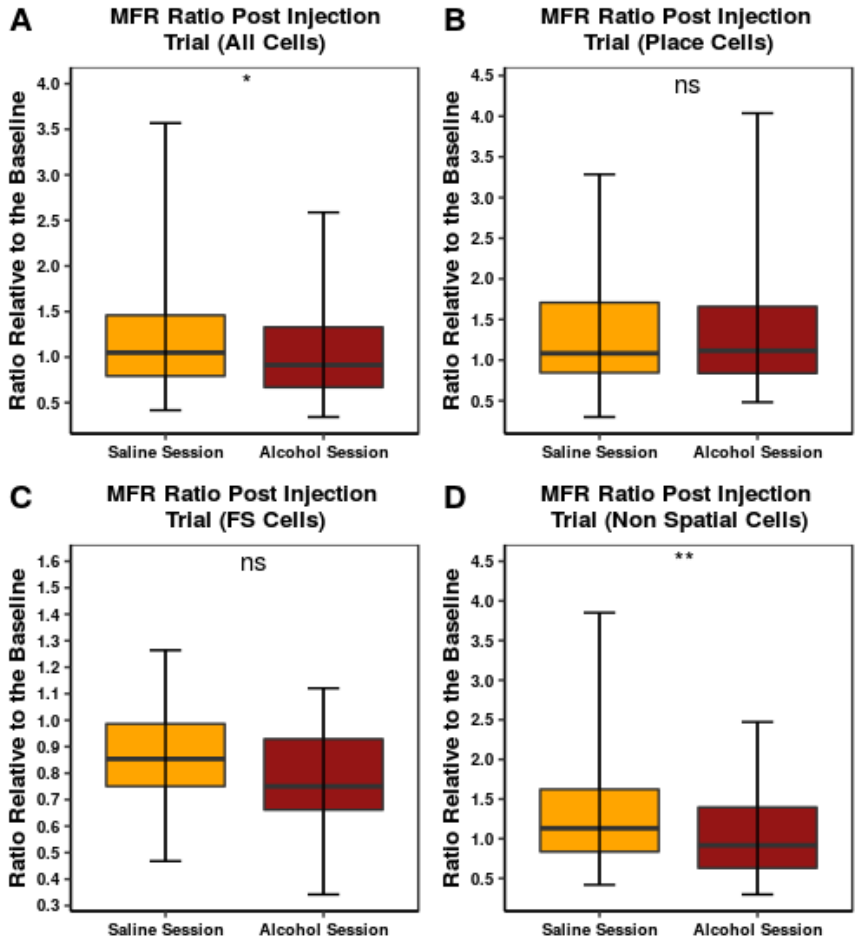

Figure 3.8: Boxplots representing the comparison of the post-injection trial MFR score ratios with respect to the baseline trial between saline session and alcohol session units. **A.** MFR of all the units pooled together. **B.** MFR of place cells. **C.** MFR of fast-spikers. **D.** MFR of non-spatial cells. A significant difference was found in the MFR ratios between saline session and alcohol session units in case of the pooled cell group and the non-spatial cell group. No significant difference was found in the MFR ratios of place cells and FS cells between saline session and alcohol session. The central bar represents the median, the whiskers represent the 5th and 95th percentile.

3.2.2 Information Score Analysis

Information score ratio of the place cells in the post-injection trial with respect to the baseline trial was investigated to determine if there was a difference between saline and alcohol sessions immediately after administering alcohol. The median saline information score ra-

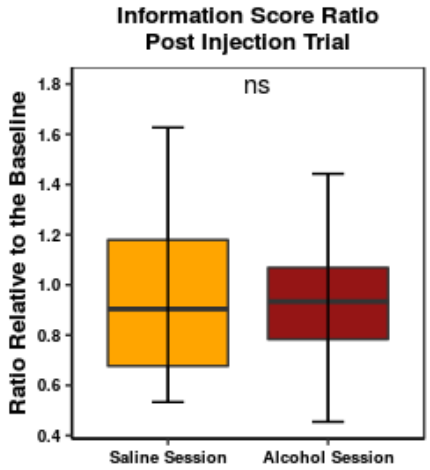

Figure 3.9: Boxplot representing the comparison of the post-injection trial information score ratio of place cells with respect to the baseline trial between saline and alcohol sessions. No significant difference was found in the information score ratio between the two sessions. The central bar represents the median, the whiskers represent the 5th and 95th percentile. ns: not significant.

tio for 47 place cells was found to be 0.90, IQR = 0.68 - 1.18 (Figure 3.9). The median for the alcohol information score ratio for 52 place cells was found to be 0.93, IQR = 0.78 - 1.07 (Figure 3.9). There was no significant difference in the information score of the place cells in the post-injection trial with respect to the baseline trial between saline and alcohol sessions (Wilcoxon rank-sum test: $p = 0.96$). Therefore, it was found that the information scores of the place cells were similar in the saline and alcohol sessions after acute alcohol intoxication. In fact, the location of the place fields also did get disrupted after acute alcohol administration (Figure 3.10).

3.2.3 LFP Theta Frequency

The LFP theta frequency ratio for the post-injection trial with respect to the baseline trial was computed to investigate if the theta frequency changes immediately after alcohol administration. The median LFP theta frequency ratio of the post-injection trial with respect to the baseline trial of 140 saline sessions was 0.99, IQR = 0.97 - 1.00 (Figure 3.11, A). The median LFP theta frequency ratio of the post-injection trial for 140 alcohol sessions was 0.93, IQR = 0.90 - 0.95 (Figure 3.11, A). There was a significant difference in the LFP theta frequency ratio of alcohol sessions as compared to the saline sessions. (Wilcoxon rank-sum test, $p < 2.2e\text{-}16$). Thus, there was a statistically significant drop in the LFP theta frequency just after i.p. administration of alcohol.

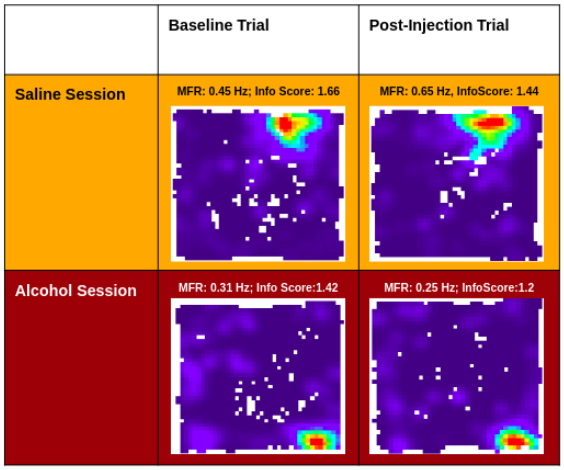

Figure 3.10: Representative examples of place cell in the post-injection trial. Firing rate maps of place cells along with trial-specific information score for a saline session and an alcohol session. The location of the place field did not change upon acute alcohol administration.

3.2.4 LFP Theta Power

The LFP theta power ratio of the post-injection trial with respect to the baseline trial was calculated to examine if the theta power was affected upon acute alcohol intoxication. The median LFP theta power ratio of the post-injection trial with respect to the baseline trial of 140 saline sessions was 0.89, IQR = 0.79 - 0.94 (Figure 3.11, B). The median LFP theta power ratio for 140 alcohol sessions was 0.82, IQR = 0.68 - 0.93 (Figure 3.11, B). There was a significant difference in the LFP theta power ratio of the alcohol sessions as compared to the saline sessions (Wilcoxon rank-sum test, p = 0.009). Thus, a statistically significant drop in the LFP theta power was observed just after injecting alcohol.

3.2.5 Speed Filtered ($\geq$5 cm/s) LFP Theta Frequency

The LFP theta frequency ratio of the post-injection trial with respect to the baseline trial after the application of the speed filter of 5 cm/s was computed to investigate if the theta frequency, while the mice were running, was differentially affected between saline and alcohol sessions upon acute alcohol intoxication. The median LFP theta frequency ratio of 120 saline sessions was 0.99, IQR = 0.97 - 1.01 (Figure 3.12, A) while the mice were running. The median LFP theta frequency ratio of 120 alcohol sessions was 0.93, IQR = 0.91 - 0.95 (Figure 3.12, A) while the mice were running. A significant difference in the LFP theta frequency ratio in the post-injection trial between the saline and alcohol

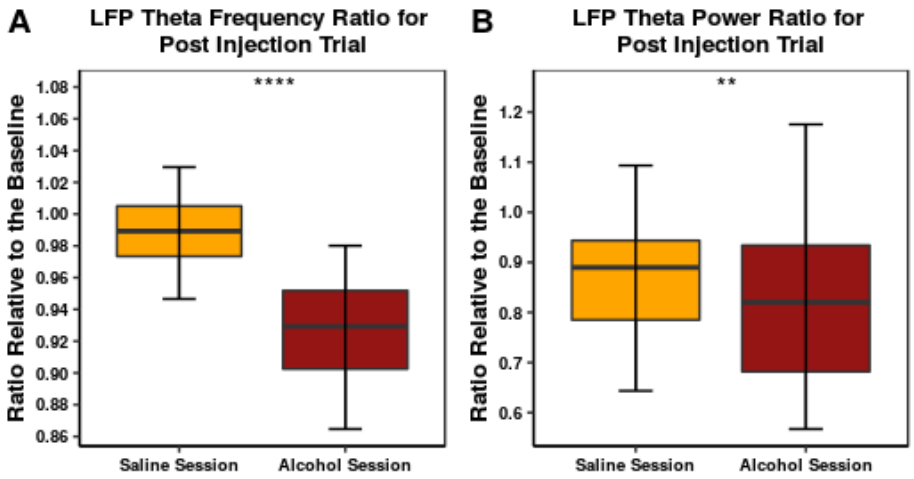

Figure 3.11: Boxplots representing the comparison of the LFP theta frequency ratio (A) and power ratio (B) of the post-injection trial with respect to the baseline trial between saline and alcohol sessions. A statistically significant difference was found between the saline and alcohol sessions in both theta frequency and power comparisons with the latter having greater lowering of both theta frequency and power in the post-injection trial. The central bar represents the median, the whiskers represent the 5th and 95th percentile.

sessions was observed (Wilcoxon rank-sum test, $p < 2.2e\text{-}16$) when the mice were running. Thus, no change was observed in the earlier observation (LFP theta frequency ratio in the post-injection trial without any speed filter) and the reduction in the LFP theta frequency following acute alcohol intoxication still remained when only the epochs where the mice were running was considered.

3.2.6 Speed Filtered ($\geq$5 cm/s) LFP Theta Power

The following analysis was performed to investigate the possible effects of running on the LFP theta power ratio of the post-injection trial with respect to the baseline trial between saline and alcohol sessions immediately after injecting saline or alcohol. The median LFP theta power ratio of 120 saline sessions was 0.97, IQR = 0.93 - 1.02 (Figure 3.12, B) while the mice were running. The median LFP theta power ratio of 120 alcohol sessions was 1.05, IQR = 0.99 - 1.10 (Figure 3.12, B) while the mice were running. A significant difference was observed in the LFP theta power ratio between the saline and the alcohol sessions with a greater increase in the relative power ratio in the alcohol sessions as compared to the saline sessions when the mice were running (Wilcoxon rank-sum test, $p = 2.07e\text{-}11$). Thus, there was a statistically significant increase in the theta power following alcohol administration when only the epochs where the mice were running was considered. This trend is in contrast

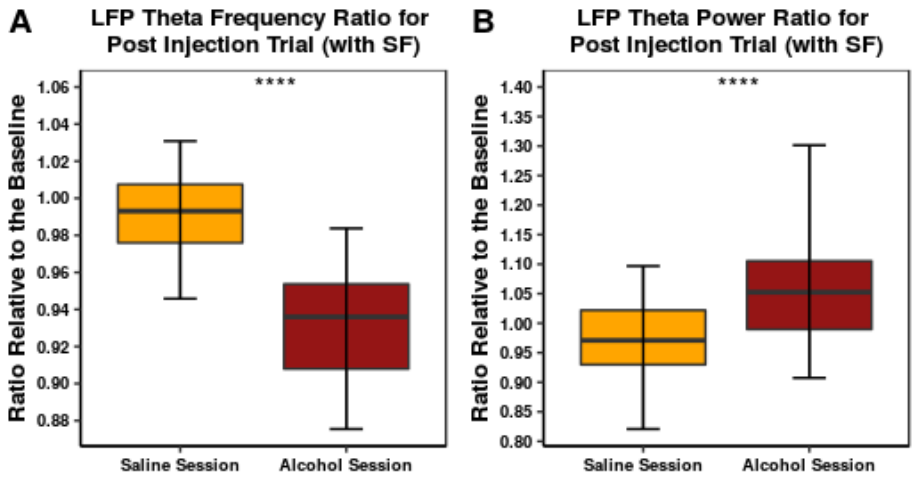

Figure 3.12: Boxplots representing the comparison of the LFP theta frequency ratio (A) and relative power ratio (B) in the post-injection trial with respect to the baseline trial between saline and alcohol sessions after applying a speed filter of 5 cm/s. A significant difference was found between the saline and alcohol sessions in both theta frequency and power comparisons. Alcohol sessions had a lowering of theta frequency ratio and an increase in the relative power ratio in the post-injection trial as compared to the saline sessions when the mice were running. The central bar represents the median, the whiskers represent the 5th and 95th percentile. SF: Speed Filter ($\geq$5 cm/s).

to what was seen in the theta power ratio in the post-injection trial without any speed filter, where the theta power ratio in saline sessions was significantly greater than the alcohol sessions.

3.2.7 Within Trial Comparison With and Without Speed Filter

The following analysis was performed to investigate if the LFP theta frequency and the LFP relative theta power showed different behaviour when the mice were running compared to the average movement speed throughout the post-injection trial in both saline and alcohol sessions. The within-trial (post-injection trial) theta frequency median values for the saline sessions were 8.09 Hz, IQR = 7.91 - 8.26 Hz (no filter); 8.11 Hz, IQR = 7.93 - 8.29 Hz (speed filter), for the alcohol sessions it was 7.64 Hz, IQR =7.35 - 7.82 (no filter) ; 7.65 Hz, IQR = 7.38 - 7.85 (speed filter). Similarly, the within-trial (post-injection trial) relative theta power median values for the saline sessions were 4.91, IQR = 4.14 - 5.83 (no filter); 6.68, IQR = 5.81 - 7.11 (speed filter) and the alcohol sessions were 4.33, IQR = 3.57 - 5.33 (no filter); 7.03, IQR = 6.10 - 7.52 (speed filter). Theta frequency was not found to be significantly different after applying a speed filter compared to when there was no speed

filter in both saline and alcohol sessions in the post-injection trials (Wilcoxon Rank Sum test, Saline: p = 0.56, Figure 3.13, A; Alcohol: p = 0.43, Figure 3.13, B). Theta power, on the other hand, was found to be significantly greater when the mice were running (with speed filter) as compared to when there was no speed filter in both saline and alcohol groups (Wilcoxon Rank Sum test, Saline: $p < 2.2e\text{-}16$, Figure 3.13, C; Alcohol: $p < 2.2e\text{-}16$, Figure 3.13, D). Therefore, there was no statistical difference in the LFP theta frequency when the mice were running compared to the average speed with which they moved throughout the post-injection trial in both saline and alcohol sessions, while there was a statistical increase in the LFP relative power when the mice were running in both saline and alcohol sessions.

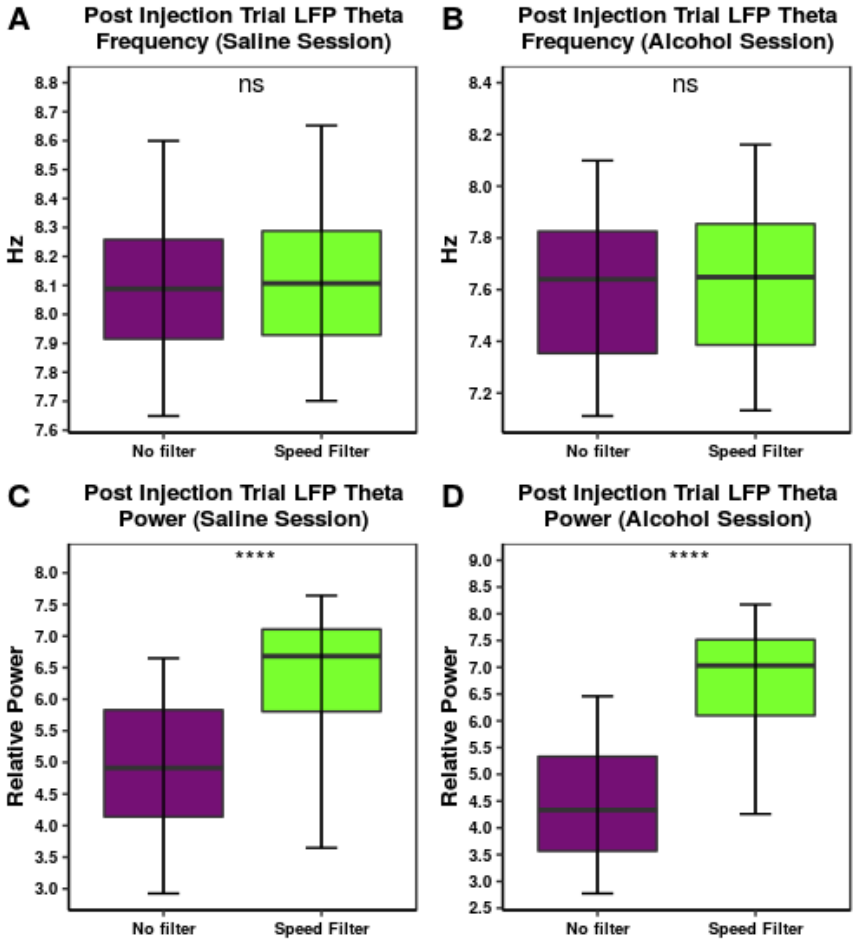

Figure 3.13: Boxplot representing the comparison of the no-speed filter and speed filter (5 cm/s) for the post-injection trial while looking at LFP theta frequency (top) and relative power(bottom) in saline (left) and alcohol (right) sessions. No statistically significant difference was found in the LFP theta frequency when the mice were running compared to their average movement speed throughout the post-injection trial in both saline **(A.)** and alcohol **(B.)** sessions. A significant increase in the relative LFP theta power was found when the mice were running in both saline **(C.)** and alcohol **(D.)** sessions. The central bar represents the median, the whiskers represent the 5th and 95th percentile.

3.3 Septum Stimulation Trial

3.3.1 Mean Firing Rate Analysis

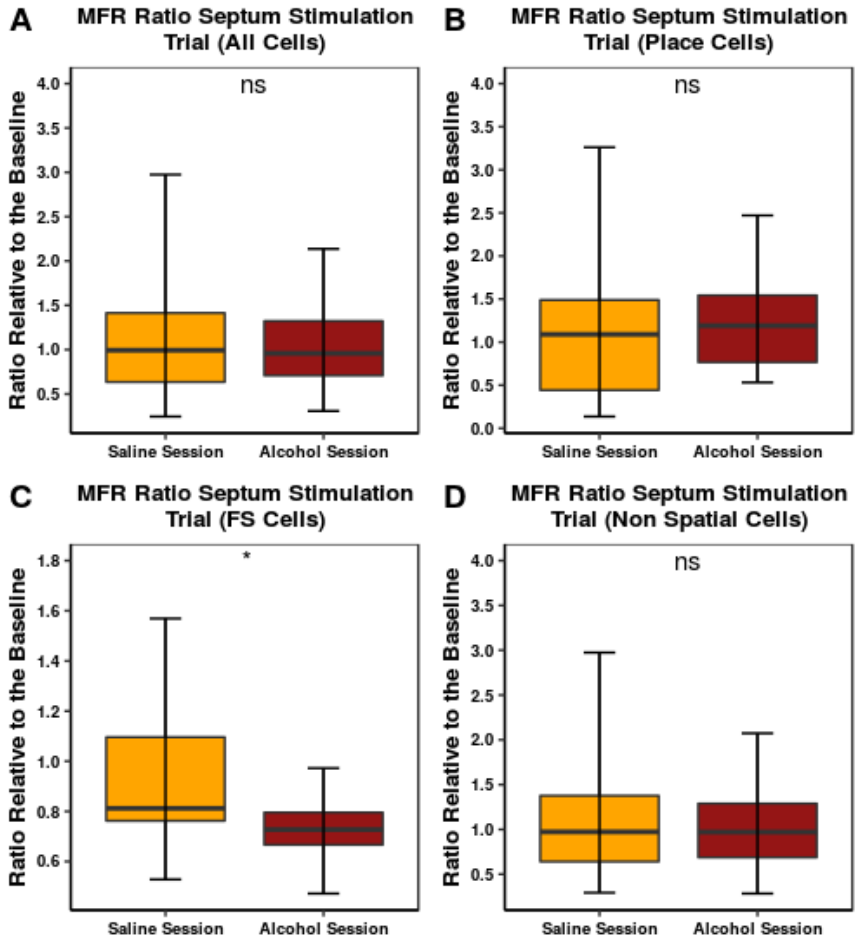

Figure 3.14: Boxplots representing the comparison of the MFR score ratios between saline session and alcohol session units in septum stimulation trial with respect to the baseline trial. A. MFR of all the units pooled together. **B.** MFR of place cells. **C.** MFR of fast-spikers. **D.** MFR of non-spatial cells. A significant difference was found in the MFR ratios between saline session and alcohol session units in case of the FS subpopulation. The central bar represents the median, the whiskers represent the 5th and 95th percentile.

The following analysis was carried out to examine if there was a significant difference in the MFR of the CA1 neurons between saline and alcohol sessions while PV+ cells in the MS were being optogenetically stimulated. The median saline MFR ratio of septum stimulation trial with respect to baseline trial for 114 units was found to be 0.99, IQR = 0.63 - 1.41 (Figure 3.14, A). The median alcohol MFR ratio for 117 units was found to be 0.96, IQR = 0.71 - 1.32 (Figure 3.14, A). There was no significant difference in the MFR ratios between saline session and alcohol session units (Wilcoxon rank-sum test: p = 0.98). Individual

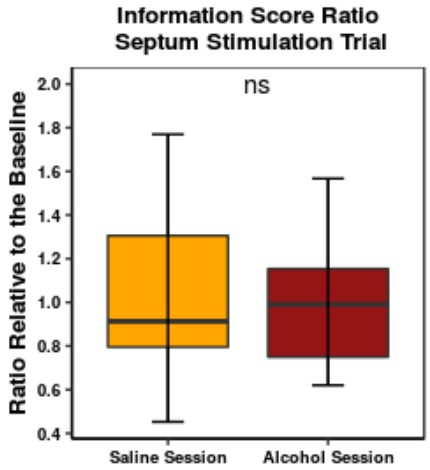

Figure 3.15: Boxplot representing the comparison of the information score ratios in the septum stimulation trial with respect to the baseline trial between saline and alcohol session place cells. No significant difference was found between the saline and alcohol sessions. The central bar represents the median, the whiskers represent the 5th and 95th percentile. ns: not significant.

subpopulations were investigated to figure out the contributions of all these groups: place cells (saline(25): median = 1.09, IQR = 0.44 - 1.49; alcohol(39): median = 1.19, IQR = 0.76 - 1.54; Figure 3.14, B), FS (saline(15): median = 0.81, IQR = 0.76 - 1.09; alcohol(18): median = 0.73, IQR = 0.67 - 0.79; Figure 3.14, C) and non-spatial cells (saline(74): median = 0.97, IQR = 0.64 - 1.38; alcohol(60): median = 0.97, IQR = 0.69 - 1.29; Figure 3.14, D). No significant difference was found in the MFR ratios between the saline and alcohol sessions in case of place cell and non-spatial cell subpopulations. A significant difference between the alcohol and saline sessions for the ratios of MFR was seen in the case of FS cells.(Wilcoxon rank-sum test, place cells: $p = 0.33$; FS cells: $p = 0.04$; non-spatial, cells: $p = 0.76$). Therefore, a statistically significant reduction in the MFR ratio of the FS cells was seen in the alcohol sessions as compared to saline sessions in the septum stimulation trial with respect to the baseline trial. No statistical difference was observed for the other cell types namely place cells and non-spatial cells for the same.

3.3.2 Information Score Analysis

Information score ratio of the place cells in the septum stimulation trial with respect to the baseline trial was investigated to determine if there was a difference in the information score of the place cells between the saline and alcohol sessions while the PV+ cells in the MS were being optogenetically stimulated. The median saline information score ratio for

25 place cells was found to be 0.91, IQR = 0.79 - 1.31 (Figure 3.15). The median alcohol information score ratio for 39 place cells was found to be 0.99, IQR = 0.75 - 1.15 (Figure 3.15). There was no significant difference in the baseline trial between saline and alcohol group units (Wilcoxon rank-sum test: p = 1). Therefore, there was no difference in the information score of place cells between saline and alcohol sessions when the PV+ cells in the MS were being optogenetically stimulated.

3.3.3 LFP Theta Frequency

The LFP theta frequency ratio for the septum stimulation trial with respect to the baseline trial was computed to investigate if the effects of alcohol intoxication on theta frequency changed while the PV+ cells in the MS were optogenetically stimulated. The median LFP theta frequency ratio of the septum stimulation trial with respect to the baseline trial of 75 saline sessions was 1.00, IQR = 0.97 - 1.04 (Figure 3.16, A). The median LFP theta frequency ratio for 75 alcohol sessions was 0.96, IQR = 0.93 - 1.00 (Figure 3.16, A). There was a significant difference in the LFP theta frequency ratio in the septum stimulation trial with respect to the baseline trial between saline and alcohol sessions (Wilcoxon rank-sum test, p = 0.0003). Therefore, the LFP theta frequency was still significantly lower in the alcohol sessions as compared to the saline sessions while the PV+ cells in the septum were being stimulated.

3.3.4 LFP Theta Power

The following analysis was performed to investigate if the stimulation of PV+ cells in the MS differentially affected the LFP theta power in the saline and alcohol sessions. This was done by looking at the LFP theta power ratio of the septum stimulation trial with respect to the baseline trial in these sessions. The median LFP theta power ratio of the septum stimulation trial with respect to the baseline trial of 75 saline sessions was 0.66, IQR = 0.55 - 0.82 (Figure 3.16, B). The median LFP theta power ratio for 75 alcohol sessions was 0.73, IQR = 0.54 - 0.90 (Figure 3.16, B). There wasn't any significant difference in the LFP theta power ratio in the septum stimulation trial with respect to the baseline trial between saline and alcohol sessions (Wilcoxon rank-sum test, p = 0.45). Thus, the LFP theta power in the septum stimulation trial was found to be similar in both saline and alcohol sessions while

the PV+ cells in the MS were being optogenetically stimulated.

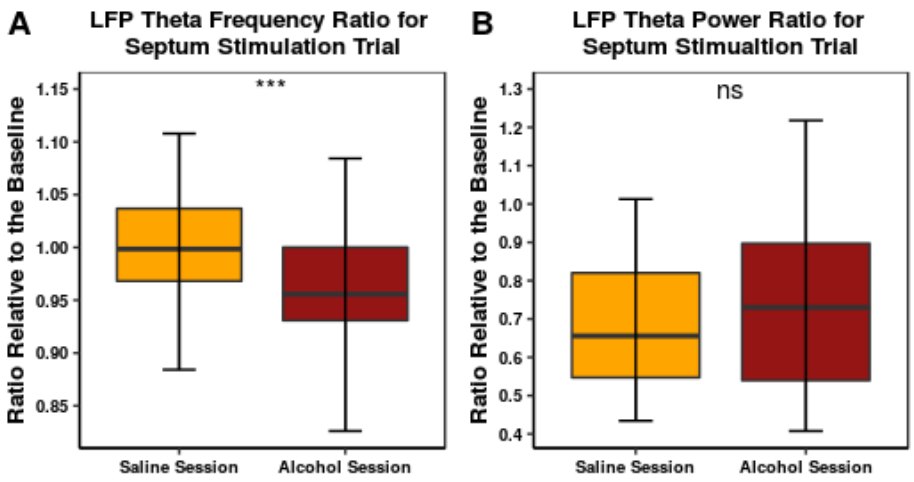

Figure 3.16: Boxplots representing the comparison of the LFP theta frequency ratio (A) and power ratio (B) in the septum stimulation trial with respect to the baseline trial between saline and alcohol sessions A significant difference was found between the two sessions in case of theta frequency ratios with the alcohol sessions having a greater lowering of theta frequency than saline sessions. No significant difference was found in the relative power ratio between the two sessions. The central bar represents the median, the whiskers represent the 5th and 95th percentile. ns: not significant.

3.3.5 Speed Filtered ($\geq$5 cm/s) LFP Theta Frequency

The LFP theta frequency ratio for the septum stimulation trial with respect to the baseline trial was computed to investigate if the effects of alcohol intoxication on theta frequency when the mice were running changed upon stimulation of the PV+ cells in the MS. The median LFP theta frequency ratio of the septum stimulation trial with respect to the baseline trial of 56 saline sessions was 1.01, IQR = 0.98 - 1.03 (Figure 3.17, A) while the mice were running. The median LFP theta frequency ratio of the septum stimulation trial with respect to the baseline trial of 56 alcohol sessions was 0.96, IQR = 0.94 - 0.98 Hz (Figure 3.17, A) while the mice were running. A significant difference in the LFP theta frequency ratio between the two sessions was observed after applying the speed filter (Wilcoxon rank-sum test, p = 2.99e-10). Thus, as with no filter, the theta frequency was significantly lower in the alcohol sessions as compared to the saline sessions while the mice were running upon stimulating the PV+ cells in the septum.

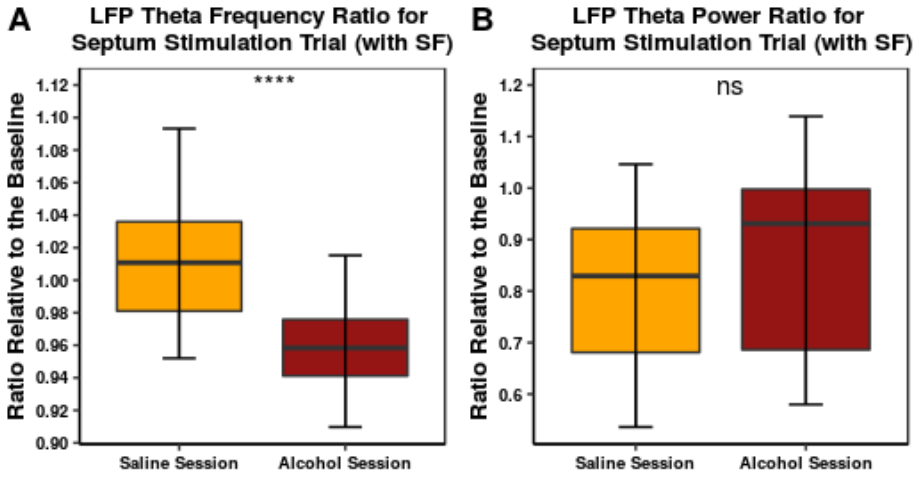

Figure 3.17: Boxplots representing the comparison of the LFP theta frequency ratio (A) and relative power ratio (B) in the septum stimulation trial with respect to the baseline trial between saline and alcohol sessions after applying a speed filter of 5 cm/s. A significant difference was found between the saline and alcohol sessions in case of theta frequency ratio with the alcohol sessions having lower theta frequency ratio than the saline sessions while the mice were running in the septum stimulation trial. No significant difference was found in the relative power ratio between the two sessions while the mice were running in the septum stimulation trial. The central bar represents the median, the whiskers represent the 5th and 95th percentile. SF: Speed Filter ($\geq$5 cm/s).

3.3.6 Speed Filtered ($\geq$5 cm/s) LFP Theta Power

The LFP theta power ratio for the septum stimulation trial with respect to the baseline trial was calculated to investigate the differences in the theta power between the saline and alcohol sessions when the mice were running and upon optogenetic stimulation of the PV+ cells in the MS. The median LFP theta power ratio of the septum stimulation trial with respect to the baseline trial of 56 saline sessions was 0.83, IQR = 0.68 - 0.92 (Figure 3.17, B) while the mice were running. The median LFP theta power ratio of the septum stimulation trial with respect to the baseline trial of 56 alcohol sessions was 0.93, IQR = 0.69 - 1.00 (Figure 3.17, B) while the mice were running. It was observed that the median of theta power ratio while the mice were running was greater in the alcohol sessions as compared to the saline sessions in the septum stimulation trial with respect to the baseline trial. However, this difference wasn't significant (Wilcoxon rank-sum test, p = 0.053). Therefore, the LFP theta power was found to be similar in both saline and alcohol sessions in the septum stimulation trial while the mice were running and the PV+ cells in the septum were being stimulated.

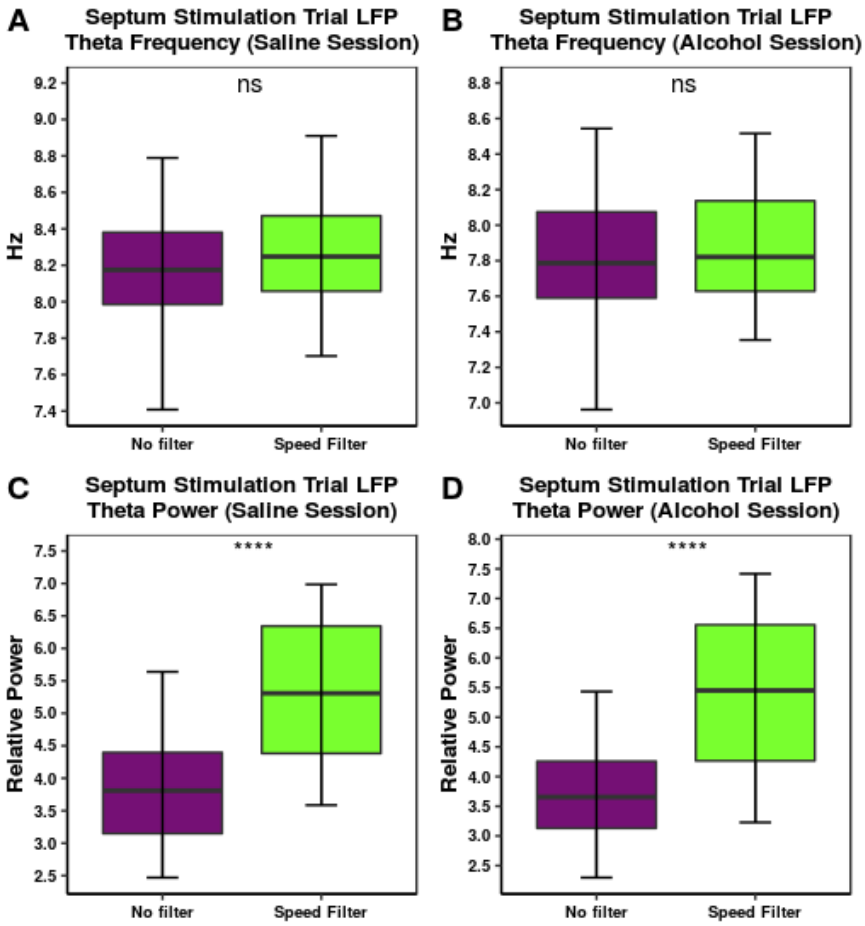

Figure 3.18: Boxplot representing the comparison of the no-speed filter and speed filter (5 cm/s) for the septum stimulation trial while looking at LFP theta frequency (top) and relative power(bottom) in saline (left) and alcohol (right) sessions. No statistically significant difference was found in the LFP theta frequency when the mice were running compared to their average movement speed throughout the septum stimulation trial in both saline **(A.)** and alcohol **(B.)** sessions. A significant increase in the relative LFP theta power was found when the mice were running in both saline **(C.)** and alcohol **(D.)** sessions. The central bar represents the median, the whiskers represent the 5th and 95th percentile.

3.3.7 Within Trial Comparison With and Without Speed Filter

The following analysis was performed to investigate if the LFP theta frequency and the LFP relative theta power showed different behaviour when the mice were running compared to their average movement speed throughout the septum stimulation trial in both saline and alcohol sessions. The within-trial (septum stimulation trial) theta frequency median values for the saline sessions were 8.17 Hz, IQR = 7.98 - 8.38 Hz (no filter); 8.25 Hz, IQR = 8.06 - 8.47 Hz (speed filter), for the alcohol sessions they were 7.79 Hz, IQR = 7.59 - 8.07 (no filter); 7.82 Hz, IQR = 7.63 - 8.14 (speed filter). Similarly, the within-trial (septum

stimulation trial) relative theta power median values for the saline sessions were 3.81, IQR = 3.15 - 4.40 (no filter); 5.31, IQR = 4.38 - 6.34 (speed filter) and the alcohol sessions were 3.66, IQR = 3.13 - 4.26 (no filter); 5.45, IQR = 4.27 - 6.56 (speed filter). Theta frequency was not found to be significantly different after applying a speed filter compared to when there was no speed filter in both saline and alcohol sessions in the septum stimulation trials (Wilcoxon rank-sum test, Saline: p = 0.16, Figure 3.18, A; Alcohol: p = 0.42, Figure 3.18, B). Relative theta power, on the other hand, was found to be significantly greater when the mice were running (with speed filter) as compared to when there was no speed filter in both saline and alcohol sessions (Wilcoxon rank-sum test, Saline: p = 2.01e-9, Figure 3.18, C; Alcohol: p = 2.41e-9, Figure 3.18, D). Therefore, there was no statistical difference in the LFP theta frequency when the mice were running compared to the average speed with which they moved throughout the septum stimulation trial in both saline and alcohol sessions, while there was a statistically significant increase in the LFP relative power when the mice were running in both saline and alcohol sessions while the PV+ cells in the MS were being optogenetically stimulated.

3.4 Recovery Trials

3.4.1 Mean Firing Rate Analysis

The following analysis was carried out to investigate if there was a significant difference in the MFR of the CA1 neurons between saline and alcohol sessions in the recovery trial. The median MFR ratio of the recovery trial with respect to the baseline trial for 114 units in the saline session was found to be 0.96, IQR = 0.64 - 1.26 (Figure 3.19, A). The median MFR ratio of the recovery trial with respect to the baseline trial for 117 units in the alcohol session was found to be 0.86, IQR = 0.68 - 1.34 (Figure 3.19, A). There was no significant difference in the MFR ratios between saline session and alcohol session units (Wilcoxon rank-sum test: p = 0.75). Individual subpopulations were investigated to find the contributions of all these groups: place cells (saline(25): median = 0.96, IQR = 0.36 - 1.46; alcohol(39): median = 1.24, IQR = 0.79 - 1.55; Figure 3.19, B), FS (saline(15): median = 0.82, IQR = 0.71 - 1.03; alcohol(18): median = 0.73, IQR = 0.71 - 0.81; Figure 3.19, C) and non-spatial cells (saline(74): median = 0.97, IQR = 0.72 - 1.26; alcohol(60): median = 0.83, IQR = 0.59 - 1.29; Figure 3.19, D). No significant difference was found in the MFR

ratios in the recovery trial with respect to the baseline trial between the saline and alcohol sessions in any of the subpopulations (Wilcoxon rank-sum test, place cells: $p = 0.13$; FS cells: $p = 0.08$; non-spatial cells: $p = 0.30$). Therefore, the MFR of the subpopulations were similar between saline and alcohol sessions in the recovery trial.

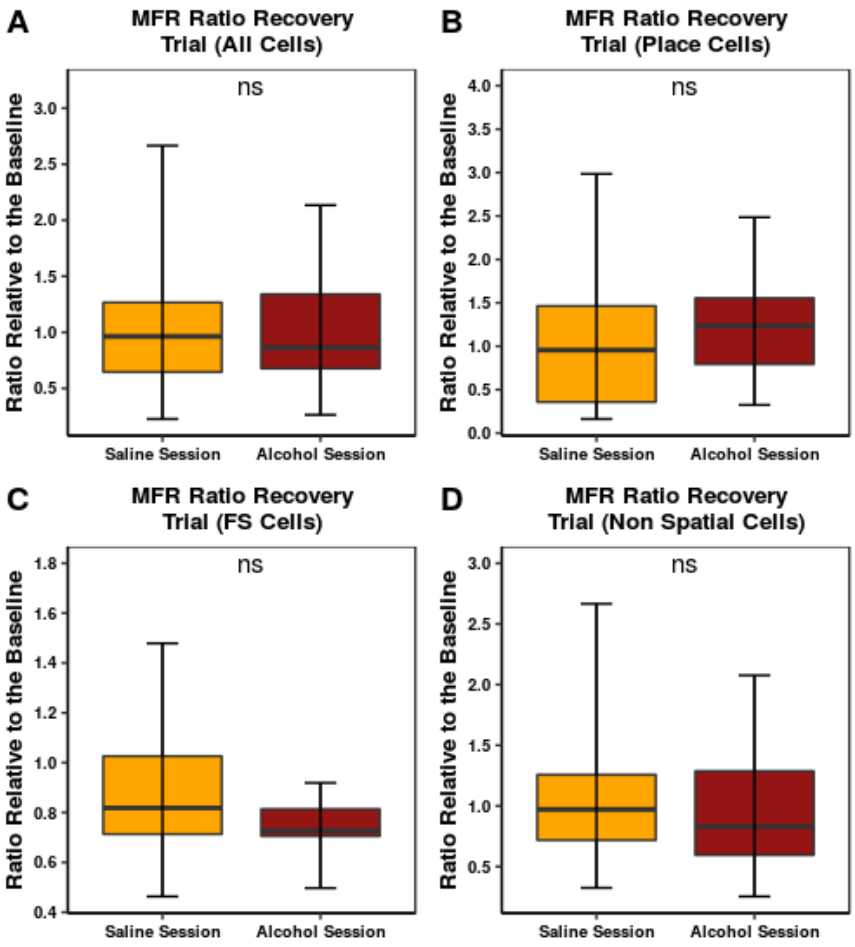

Figure 3.19: Boxplots representing the comparison of the MFR score ratios in the recovery trial with respect to the baseline trial between saline session and alcohol session units. **A.** MFR of all the units pooled together. **B.** MFR of place cells. **C.** MFR of fast-spikers. **D.** MFR of non-spatial cells. No significant difference was found in the MFR ratios between saline and alcohol session units for the pooled as well as for individual subpopulations. The central bar represents the median, the whiskers represent the 5th and 95th percentile. ns: not significant.

3.4.2 Information Score Analysis

Information score ratio of the place cells in the recovery trial with respect to the baseline trial was investigated to determine if there was a difference in the information score of the place cells between the saline and alcohol sessions in the recovery trial. The median saline

information score ratio for 25 place cells was found to be 0.88, IQR = 0.72 - 1.08 (Figure 3.20). The median alcohol information score ratio for 39 place cells was found to be 0.89, IQR = 0.70 - 1.10 (Figure 3.20). There was no significant difference in the information score ratio of the place cells in the recovery trial with respect to the baseline trial between saline and alcohol sessions (Wilcoxon rank-sum test: p = 0.96). Thus, the information score of place cells was similar in saline and alcohol sessions in the recovery trial.

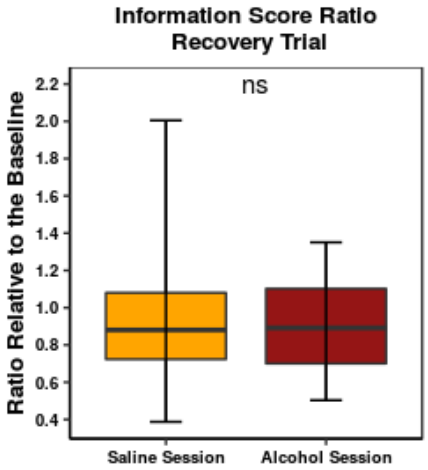

Figure 3.20: Boxplot representing the comparison of the information score ratios in the recovery trial with respect to the baseline trial between saline and alcohol session place cells. No significant difference was found between the two session place cells. The central bar represents the median, the whiskers represent the 5th and 95th percentile. ns: not significant.

3.4.3 LFP Theta Frequency

The LFP theta frequency ratio for the recovery trial with respect to the baseline trial was computed to investigate if the effects of alcohol intoxication on theta frequency still persisted in the recovery trial. The median LFP theta frequency ratio of the recovery trial with respect to the baseline trial for 75 saline sessions was 1.01, IQR = 0.99 - 1.03 (Figure 3.21, A). The median LFP theta frequency ratio of the recovery trial with respect to the baseline trial for 75 alcohol sessions was 0.98, IQR = 0.95 - 1.00 (Figure 3.21, A). There was a significant difference in the LFP theta frequency ratio in the recovery trial with respect to the baseline trial between saline and alcohol sessions (Wilcoxon rank-sum test, $p < 5.77e\text{-}5$). Therefore, a statistically significant drop in the LFP theta frequency in the alcohol sessions as compared to the saline sessions still persisted in the recovery trial.

3.4.4 LFP Theta Power

The LFP theta power ratio for the recovery trial with respect to the baseline trial was computed to investigate if there was a difference in the theta power between saline and alcohol sessions in the recovery trial. The median LFP theta power ratio of the recovery trial with respect to the baseline trial of 75 saline sessions was 0.87, IQR = 0.74 - 0.96 (Figure 3.21, B). The median LFP theta power ratio of the recovery trial with respect to the baseline trial for 75 alcohol sessions was 0.84, IQR = 0.73 - 0.97 (Figure 3.21, B). No significant difference was observed in the LFP theta power ratio of the alcohol sessions as compared to the saline sessions (Wilcoxon rank-sum test, p = 0.76). Therefore, the LFP theta power was similar in both saline and alcohol sessions in the recovery trial.

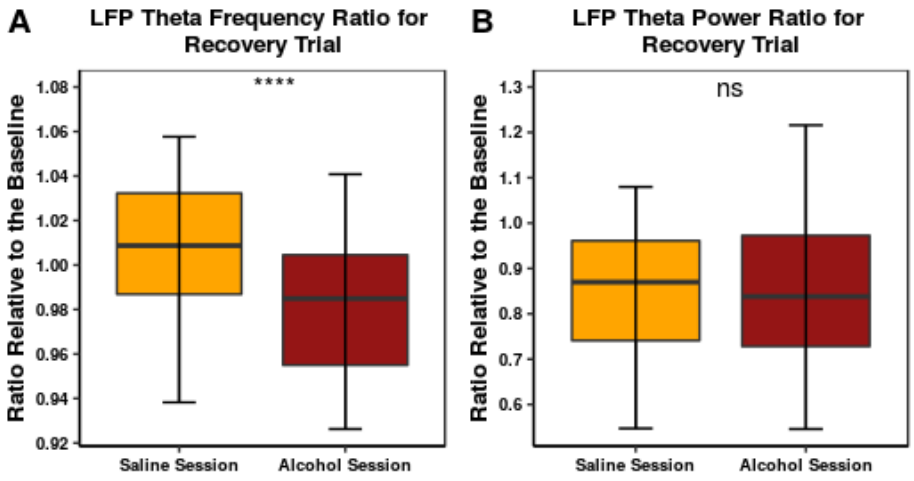

Figure 3.21: Boxplots representing the comparison of the LFP theta frequency ratio (A) and power ratio (B) in the recovery trial with respect to the baseline trial between saline and alcohol sessions. A significant difference was found between the two sessions in case of the theta frequency ratio with the alcohol sessions having a greater lowering of theta frequency in the recovery trial. No significant difference was found in the relative power ratio between the two sessions. The central bar represents the median, the whiskers represent the 5th and 95th percentile. ns: not significant.

3.4.5 Speed Filtered ($\geq$5 cm/s) LFP Theta Frequency

The following analysis was performed to investigate if the effects of alcohol intoxication on theta frequency still persisted in the recovery trial when the mice were running. The median LFP theta frequency ratio in the recovery trial with respect to the baseline trial of 56 saline sessions was 1.02, IQR = 1.00 - 1.04 (Figure 3.22, A) while the mice were running. The median LFP theta frequency ratio in the recovery trial with respect to the baseline trial of 56

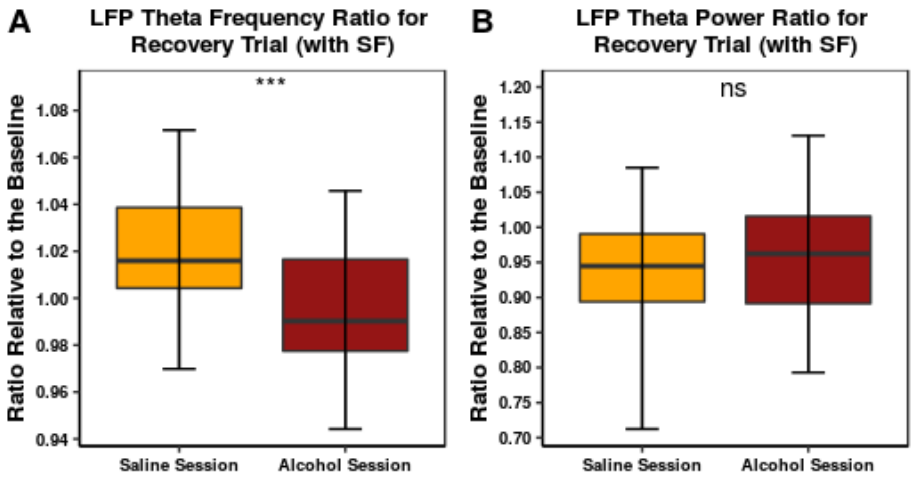

Figure 3.22: Boxplots representing the comparison of the LFP theta frequency ratio (A) and relative power ratio (B) in the recovery trial with respect to the baseline trial between saline and alcohol sessions after applying a speed filter of 5 cm/s. A significant difference was found between the two sessions in case of theta frequency ratio with the alcohol sessions having a lower theta frequency ratio compared to saline sessions while the mice were running. No significant difference was found in the relative power ratio between the two sessions while the mice were running. The central bar represents the median, the whiskers represent the 5th and 95th percentile. SF: Speed Filter ($\geq$5 cm/s).

alcohol sessions was 0.99, IQR = 0.98 - 1.02 (Figure 3.22, A) while the mice were running. A significant difference in the LFP theta frequency ratio between the two sessions was seen after applying the speed filter of 5 cm/s in the recovery trial with respect to the baseline trial (Wilcoxon rank-sum test, p = 0.0002). Thus, the drop in the LFP theta frequency due to alcohol administration still persisted in the recovery trial while the mice were running.

3.4.6 Speed Filtered ($\geq$5 cm/s) LFP Theta Power

The LFP theta power ratio for the recovery trial with respect to the baseline trial was computed to investigate if there was a difference in the theta power between saline and alcohol sessions in the recovery trial while the mice were running. The median LFP theta power ratio in the recovery trial with respect to the baseline trial of 56 saline sessions was 0.94, IQR = 0.89 - 0.99 (Figure 3.22, B) while the mice were running. The median LFP theta power ratio in the recovery trial with respect to the baseline trial of 56 alcohol sessions was 0.96, IQR = 0.89 - 1.02 (Figure 3.22, B) while the mice were running. No significant difference was observed in the LFP theta power ratio between the two sessions in the recovery trial with respect to the baseline trial after applying a speed filter of 5 cm/s (Wilcoxon rank-sum

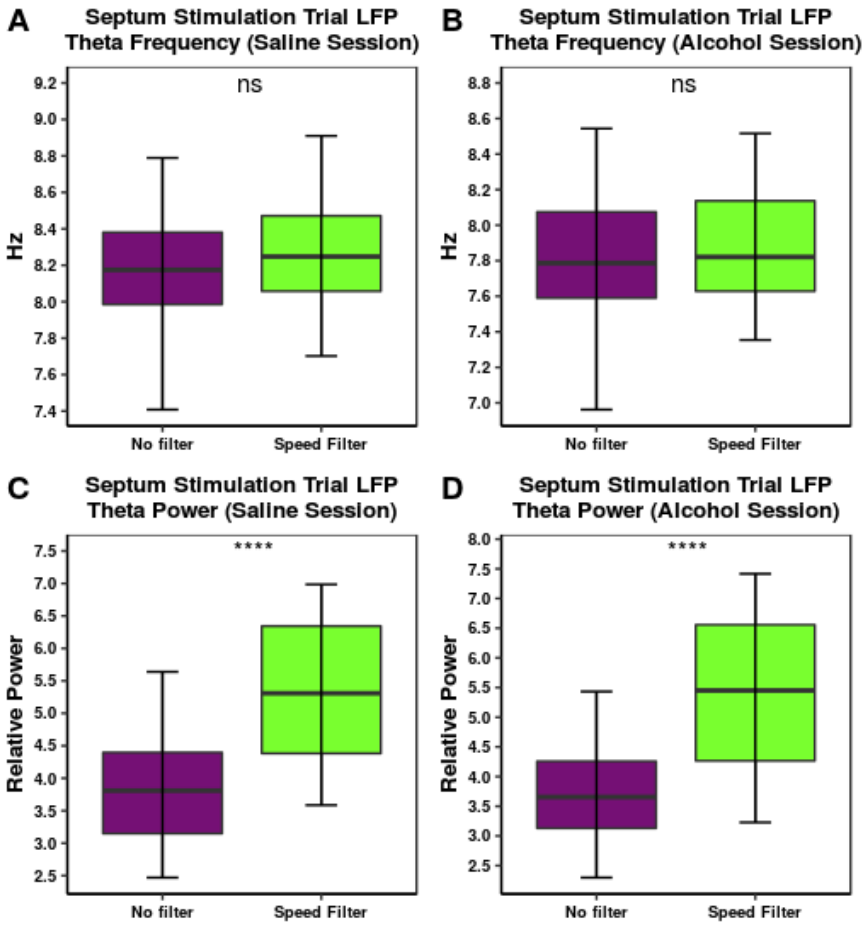

Figure 3.23: Boxplot representing the comparison of the no-speed filter and speed filter (5 cm/s) for the recovery trial while looking at LFP theta frequency (top) and relative power(bottom) in saline (left) and alcohol (right) sessions. No statistically significant difference was found in the LFP theta frequency when the mice were running compared to their average movement speed throughout the recovery trial in both saline **(A.)** and alcohol **(B.)** sessions. A significant increase in the relative LFP theta power was found when the mice were running in both saline **(C.)** and alcohol **(D.)** sessions. The central bar represents the median, the whiskers represent the 5th and 95th percentile.

test, p = 0.33). Thus, the LFP theta power was similar in both saline and alcohol sessions in the recovery trial while the mice were running.

3.4.7 Within Trial Comparison With and Without Speed Filter

The following analysis was performed to investigate if the LFP theta frequency and the LFP relative theta power showed different trends when the mice were running compared to their average movement speed throughout the recovery trial in both saline and alcohol sessions. The within-trial (recovery trial) theta frequency median values for the saline sessions were

8.29 Hz, IQR = 8.12 - 8.45 Hz (no filter); 8.33 Hz, IQR = 8.17 - 8.52 Hz (speed filter), for the alcohol sessions they were 8.15 Hz, IQR =7.93 - 8.30 Hz (no filter); 8.20 Hz, IQR = 8.01 - 8.36 Hz (speed filter). Similarly, the within-trial (recovery trial) relative theta power median values for the saline sessions were 4.55, IQR = 3.63 - 5.29 (no filter); 6.49, IQR = 5.29 - 6.92 (speed filter) and the alcohol sessions were 3.94, IQR = 3.30 - 5.23 (no filter); 6.36, IQR = 4.98 - 6.85 (speed filter). Theta frequency was not found to be significantly different after the application of the speed filter compared to when there was no speed filter in both saline and alcohol sessions in the recovery trial (Wilcoxon rank-sum test, Saline: p = 0.38, Figure 3.23, A; Alcohol: p = 0.42, Figure 3.23, B). Theta power, on the other hand, was found to be significantly greater when the mice were running (with speed filter) as compared to when there was no speed filter in both saline and alcohol sessions (Wilcoxon rank-sum test, Saline: p = 7.94e-9, Figure 3.23, C; Alcohol: p = 2.77e-10, Figure 3.23, D). Therefore, there was no statistical difference in the LFP theta frequency when the mice were running compared to the average speed with which they moved throughout the recovery trial in both saline and alcohol sessions, while there was a statistically significant increase in the LFP relative power when the mice were running in both saline and alcohol sessions in the recovery trial.

3.5 Result Summary

1. **Baseline Trial Analyses:** Mean Firing Rate analysis, Information Score Analysis and LFP theta frequency and relative power analysis between the saline and the alcohol sessions showed no statistical difference in the baseline trial. Hence, in the subsequent trials, the comparison between these two sessions by comparing the ratios of these parameters with respect to the baseline was justified.

2. **MFR Ratio Analysis:** A statistically significant drop in the MFR ratios of all pooled cells in case of alcohol session was observed in the post-injection trial. Upon investigating it further, it was found that this difference was predominantly coming from the non-spatial pyramidal neurons. There was a drop in FS cells in alcohol sessions as well, though it was not statistically significant. A significant reduction was seen only in the MFR ratio of the FS cells in the case of septum stimulation trial for alcohol sessions as compared to saline sessions. However, the number of FS cells were too

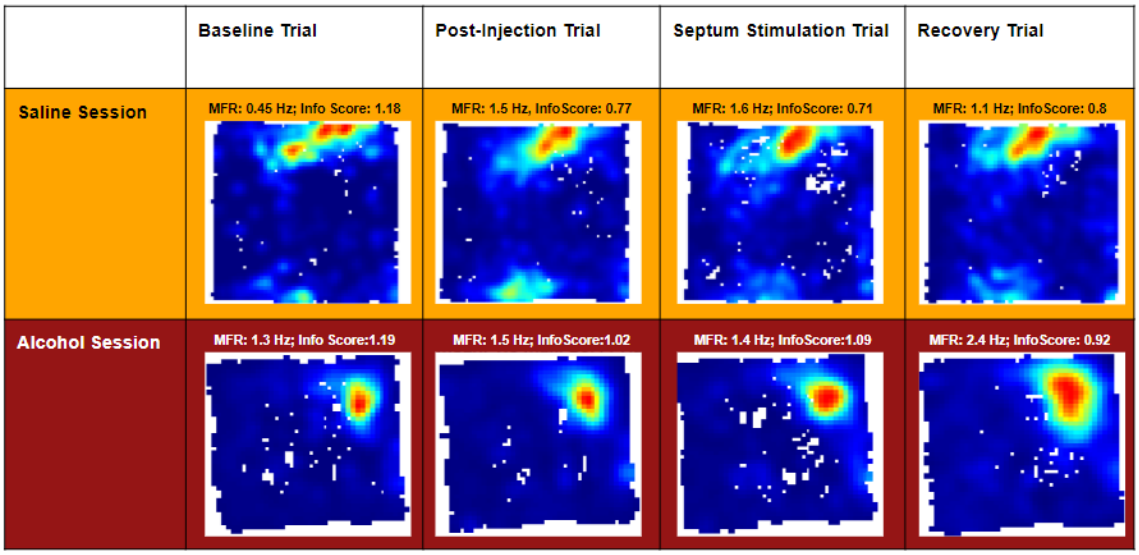

Figure 3.24: Spatial firing properties of hippocampal place cells. Firing rate maps of place cells along with trial-specific information score for a saline session and an alcohol session.

low to reliably make any conclusions.

3. **Information Score Ratio Analysis:** No significant difference between alcohol and saline sessions was found for information score ratios for any of the trials. This was also validated by visual inspection of the place fields whose spatial selectivity did not seem to get affected under the influence of alcohol (Figure 3.24).

4. **LFP Theta Frequency Ratio Analysis:** A statistically significant drop in the theta frequency in the alcohol sessions as compared to the saline sessions was observed in all the three trials after administering alcohol (Figure 3.25). This result was surprising for the stimulation of the PV+ cells in the septum trial where it suggested that a reduction in the LFP theta frequency was present for the alcohol sessions as compared to saline sessions even when the same stimulation frequency was used in both the sessions. Further, the fact that a drop in theta frequency was maintained even in the recovery trial in the alcohol sessions showed that the possible effect of alcohol was still present in that trial.

5. **Relative LFP Theta Power Ratio Analysis:** A significant reduction in the theta power of the alcohol group as compared to the saline group was observed only in the post-injection trial (Figure 3.25).

6. **Effect of Running (Speed Filter $\geq$ 5 cm/s) on the Theta Frequency Ratio (Com-**

parison Between Saline and Alcohol Sessions): In case of theta frequency ratio a lower theta frequency ratio in the alcohol sessions compared to saline sessions was observed in all the trials while the mice were running, similar to what was observed without any speed filter.

7. **Effect of Running (Speed Filter $\geq$ 5 cm/s) on the Relative LFP Theta Power Ratio (Comparison Between Saline and Alcohol Sessions):** There was a statistically significant increase in the relative theta power ratio of the alcohol group as compared to the saline group in the post-injection trial when the mice were running. The relative theta power ratio was higher in the alcohol sessions in the septum stimulation trial as well after applying a speed filter of 5cm/s though not statistically significant. There was no significant difference in the relative theta power ratio between the saline and alcohol sessions in the recovery trial while the mice were running.

8. **Effect of the Running (Speed Filter >= 5 cm/s) on the Theta Frequency Within The Same Trial (Comparison Between No Filter and Speed Filter Groups):** There was no significant difference between speed filter (when the mice were running) and no filter group in case of theta frequency across all the trials for both saline and alcohol sessions.

9. **Effect of the Running (Speed Filter >= 5 cm/s) on the Relative Theta Power Within The Same Trial (Comparison Between No Filter and Speed Filter Groups):** A statistically significant increase in the relative theta power was always seen in the case of speed filter (when the mice were running) group as compared to no filter group across all the trials for both saline and alcohol sessions.

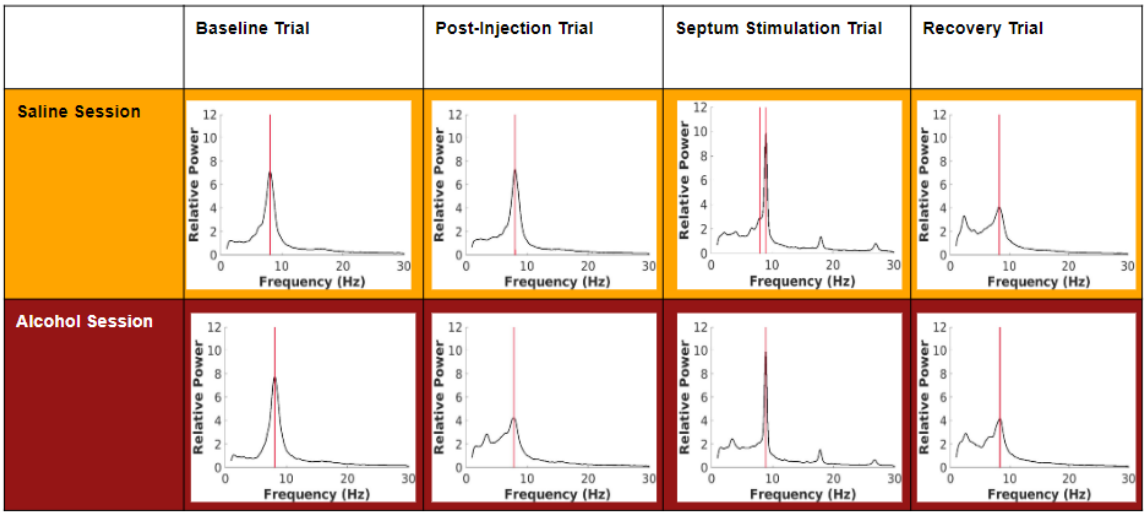

Figure 3.25: LFP theta under saline and alcohol conditions Representative example of the change in the theta frequency and power across trials for a saline session and an alcohol session. The red line represents the theta frequency with maximum power. The two red lines represent the endogenous peak and the artificially stimulated laser peak (dominant) upon septum stimulation in saline session. The endogenous peak completely overlaps the artificially stimulated laser peak in the septum stimulation trial of the alcohol session.

Chapter 4

Discussion

Spatial memory, which can be a kind of episodic memory is critical for efficiently navigating through an environment. It is known that acute alcohol intoxication causes deficits in spatial memory (*80*). The present study looked at the effects of alcohol on the unit firing and the LFP theta rhythm in the CA1 region of the hippocampus. It is the first in vivo electrophysiological study in mice to study the effect of acute alcohol intoxication on the CA1 region of the hippocampus. The previous studies used rats as their model organisms (*70–72*, *81*, *82*). Further, it is the first study to integrate optogenetic stimulation of PV+ cells in the medial septum post alcohol administration into a single paradigm to examine if the effects of alcohol on the cellular and network level could be reversed.

It has been reported that rodents could not perform memory tasks at the administered dose of alcohol, i.e. 1.5 g/kg (*72*, *77*). This was further validated by unpublished data from the present lab (personal communication), which found that the performance of mice on a spatial memory task on a radial arm maze was impaired under alcohol intoxication at concentrations of 1.0; 1.5; 2.0 g/kg. Thus deficits in spatial memory in mice should be evident at the dosage used in the present study.

4.1 Electrophysiological Changes at the Cellular Level

In the present study, it was found that the mean firing rate (MFR) of place cells did not decrease immediately following alcohol administration in the post-injection trial, nor did it drop later. Further, the information score, a measure for spatial specificity also did not drop after acute alcohol intoxication. However, a significant drop was observed in the non-spatial

pyramidal neurons immediately after injecting alcohol. The present findings are interesting in light of the previous studies. One of these reported a reduction in the overall rate of the place cell upon 1.5 g/kg i.p. administration of alcohol in awake, freely behaving rats on a Y maze (*72*). Further, the study also showed a reduction in the place cell specificity which was defined as the ratio of in-field to out-field firing rates (the in-field firing rates decreased whereas the out-field firing rates did not). Another study that used a slightly higher alcohol dosage of 2 g/kg (injected i.p.) also showed a decrease in the place cell specificity in awake, freely behaving rats on a radial arm maze (*71*). In this study, the place cell specificity was defined as the ratio of the firing rate of the neuron in the place field divided by the mean firing rate. The location of the place fields nonetheless remained stable in these studies and the same was observed in the present study (*71*, *72*). In two other studies, which used ip injection and intrahippocampal dialysis as the means of administering alcohol in awake behaving rats, a reduction in the firing rates of the pyramidal neurons in the CA1 region of the hippocampus was found (*81*, *82*). In anaesthetized rats also, a decrease in the firing rates of pyramidal neurons was found upon ip administration of alcohol (*70*).

The reduction in the MFR of the place cells and the reduction in the spatial selectivity following acute alcohol administration witnessed in some studies (*71*, *72*) had one major difference in terms of the experimental paradigm from the one used in the present study. In both of these studies, maze tasks were used as opposed to random foraging task as the behavioural paradigm. It is known that goal-directed behaviour boosts in-field behaviour, which might not happen in the random foraging tasks especially when the reward distribution is uniform which was the case in the present study (*11*). This might explain why the MFR and the information score did not decrease following acute alcohol administration in the present study. It is also to be noted that in the study (*70*), the experiment was performed while the rats were anaesthetized. It has been shown that anaesthetics interact with alcohol and may obscure some aspects of its cellular effects (*83*, *84*). In another recent study (*82*), which looked at the effects of acute alcohol on the hippocampus, the rats were not freely moving even though they were awake and behaving. Therefore, the results of this study might not reflect what happens to place cells when the rodents are actively engaged in moving around. Further, in a study in which alcohol was administered via intrahippocampal microdialysis (*81*), different physiological effects as compared to ip administration might be seen. It is also noteworthy to mention that in these previous studies (*70*, *81*, *82*) the find-

ings were about the pyramidal cells in the CA1 region of the hippocampus and not place cells in particular. This is because, the rat's position was not correlated with their spike trains (the rats were either not moving or their path was not being recorded), and thus the spatial nature of these neurons was not confirmed. Therefore, it is likely that the recorded pyramidal neurons in these studies contained both spatial as well as non-spatial cells. It is tempting to speculate that the drop in the firing rates of the pyramidal neurons seen in these studies might be because of the non-spatial neurons, as was seen in the present study as well.

In the present study, it was observed that the MFR of FS (putative interneurons) showed a decreasing trend (though not statistically significant) following acute alcohol administration in the post-injection trial. The firing rates of the interneurons were also studied in previous studies (*70*, *72*, *82*). All of them reported no statistically significant change after administering alcohol as compared to saline. In one study (*72*), the behaviour of the interneurons was diverse with three of them showing a decrease, one increase and the remaining three with no change in the firing rate. In another study (*70*), no interneuron firing rate change was observed after alcohol administration. However, it was found that interneuron discharges in the CA1 evoked by stimulation of the Schaffer collaterals increased significantly after i.p. administration of alcohol. The stimulation of Schaffer collaterals was done to mimic the normal physiological condition since the rats were under anaesthesia. However, as discussed above, anaesthesia is thought to interact with alcohol and hence the results from this study should be interpreted with caution. Importantly, the interneurons were defined on the basis of firing rates and waveform features in these studies (*70*, *72*, *82*). But in the current study, it was done on the basis of the mean firing rate only. Thus, the differences in the result between these three studies with the present study (a statistically non-significant decreasing trend in the MFR of interneurons) could be due to differences in the definition although these results in the present study were in general agreement with the previous literature. Further, the number of interneurons studied were significantly lower in all of these previous studies as compared to the present study. Specifically, 11 interneurons were studied in one study (*72*), 17 in another study (*70*). One study, however, did not mention the number of recorded interneurons (*82*). On the other hand, in the present study 94 interneurons were recorded.

The present study found a significant reduction in the MFR of the interneurons during op-

togenetic stimulation of PV+ cells in the MS. However, this result might not have sufficient statistical power due to the low number of recorded interneurons in the septum stimulation trial. In fact, the total units recorded from the septum stimulation trial was low and hence the effects of the stimulation of the PV+ cells in the MS on these units should be interpreted with caution.

Finally, an inherent methodological bias in the present study merits consideration. In the study, since only those units which fired consistently throughout the recording session were kept for analysis, a systematic underestimation of the total number of units was inevitably done. It is possible that some cells might behave physiologically in such a way (by stopping their activity immediately following alcohol injection) but were not considered for the same reason.

4.2 Electrophysiological Changes at the Network Level

There was significant suppression of the LFP theta (both frequency and relative power) after acute alcohol exposure. Previous studies looking at the effect of acute alcohol at doses that impair hippocampal-dependent learning also found a significant reduction of the LFP theta rhythm (*74*, *82*). It has been hypothesized that the reduction in the hippocampal LFP theta after acute alcohol administration might occur due to the effects of alcohol on the septum (*75*), a structure which is thought to pace the hippocampal LFP theta (*44*). Interestingly, the drop in the LFP theta frequency remained even when the PV+ cells in the MS were stimulated. However, this was not seen in all the sessions. Visual inspection of theta frequency and power in some of the sessions did show that the optogenetic stimulation of the PV+ cells in the MS could pace the LFP theta (Figure 3.24). One likely explanation for this observation would be that the optogenetic stimulation of the PV+ cells in the MS for pacing the hippocampal LFP theta was not consistently reliable. Interestingly, it was found that the drop in the LFP theta frequency persisted even in the recovery trial, which was roughly an hour after injecting the alcohol (time difference between the post-injection trial and the recovery trial). It is well known that the concentration of alcohol injected determines the blood level (*85*) and varies in rats and mice (*86*). It was shown in one study that in rats injected with a dose of 0.56 and 0.8 g/kg alcohol ip, the blood alcohol level peaked in the first 5 to 15 minutes followed by a decline in the next 15 to 30 minutes (*85*).

In contrast, in another experiment in mice injected with alcohol ip at a dose of 3.8 g/kg, alcohol concentrations rose to a peak in about 60 min and was completely flushed out from the system within 7 hours (*86*). Since a dose of 1.5 g/kg was used in the present study, it is reasonable to assume that enough alcohol was present in the mice to produce the persistent effect of a drop in the LFP theta frequency seen in the recovery trial.

In the present study, the LFP theta frequency and the relative power within-trial were calculated when the mice were running (speed filter of $\geq$ 5 cm/s) compared to their average movement speed (no filter) throughout the trial. A consistent pattern was found across all the trials in both alcohol and saline sessions. The LFP theta frequency did not change significantly when the mice were running as compared to their average running speed, whereas the LFP relative power was always found to be significantly greater at that time. Previous literature reported an inconsistent relationship between LFP theta frequency and movement. Whereas some studies showed a positive correlation between the LFP theta frequency and movement (*87*, *88*), other studies showed that the LFP theta frequency is associated only with the speed at which voluntary movement is initiated (*89–91*). Still, others did not find any correlation between the LFP theta frequency and the speed (*92*, *93*). An analysis correlating the LFP frequency with the speed at which voluntary movement was initiated was not performed in the present study. Therefore, further studies are required to understand the relationship between LFP theta and the initial voluntary movement speed. Nevertheless, in the present study, the LFP theta frequency findings suggest no correlation between the theta frequency and high running speed ($\geq$ 5cm/s) which is consistent with the finding in the previous studies (*92*, *93*).

The relative LFP theta power (the amplitude of the LFP theta) on the other hand has been shown to be positively correlated with movement in all the previous studies (*89*, *92*, *94*, *95*). The same trend was also seen in the present study. A novel finding in the present study was an increase in the LFP theta power when the mice were running that was significantly greater in case of alcohol sessions as compared to saline sessions in the post-injection trial immediately following alcohol administration. A similar trend was seen in the septum stimulation trial though it was not statistically significant. In the case of the recovery trial, there was no difference in the LFP theta power between saline and alcohol sessions when the mice were running. The reasons for these findings are unclear but it seems likely that changes due to alcohol in the LFP theta power while the mice are running decays faster

than the general effect of alcohol on the LFP theta frequency.

4.3 Summary

The present study was the first in vivo electrophysiological study in mice that aimed to find the effects of acute alcohol intoxication on the CA1 region of the hippocampus. The study also explored if the rhythmic activation of the PV+ cells in the MS, via optogenetic stimulation could restore the function of the hippocampus under the influence of alcohol. The study found that acute alcohol intoxication at a dosage of 1.5 g/kg, administered intraperitoneally led to a reduction in the MFR of non-spatial cells immediately after the injection. No significant change was seen in the MFR and the information score of place cells and the location of the place fields remained stable as well. The MFR of the interneurons did not change significantly just after alcohol administration, though a decreasing trend was seen compared to the saline sessions. At the network level, a significant drop in the LFP theta frequency and power was seen immediately after injecting alcohol. The suppression in the LFP theta frequency persisted throughout the recording session in the alcohol injected mice. Further, the optogenetic stimulation of the PV+ cells in the MS did not reliably pace the hippocampal LFP theta since the LFP theta frequency was statistically lower in case of alcohol sessions as compared to saline sessions even while the stimulation was being done. The results in the present study at both the cellular and the network levels are broadly in agreement with the previous studies. The findings of the study are important and raise some important questions about the mechanism underlying alterations of spatial memory following alcohol intoxication.

An interesting question raised by the study is what really gets disrupted under the influence of alcohol at the cellular level if only the firing properties of non-spatial cells get reduced after acute alcohol intoxication. A possibe solution to this problem may lie in investigating these pyramidal neurons (non-spatial) in greater detail and examine their physiological functional parameters upon alcohol administration. Apart from this, other firing properties of the place cells like theta phase precession, which is thought to play an important role in episodic memory in terms of phase coding, enabling synaptic plasticity and/or sequence retrieval and prediction (*39*, *40*) should also be probed to address this question. Another possibility is that the spatial memory deficits were because of a more complex

network effect. Fast-spiking interneurons are thought to be responsible for coordinating the hippocampal network dynamics for memory consolidation (*96*). An important analysis in which the place cells, interneurons and non-spatial cells are defined on the basis of the waveform and the MFR should be done. This would lead to a more standard definition of each of these categories and would thus enhance the clarity of the results. Further, it would be revealing to see the effects of alcohol in some other memory and spatial navigation oriented systems such as the medial entorhinal cortex (MEC) and the medial septum (MS). The MEC serves as both input and output to the hippocampus and houses many spatially tuned cells such as grid cells, head direction cells and border cells (*97*). It would be interesting to explore the effects of alcohol on these spatially active cells in MEC and compare the effects with the hippocampal place cells to evaluate if they behave in a similar way. Besides, the MS plays a critical role in pacing the hippocampal theta rhythm (*23*, *41*, *44*). So, electrophysiological recordings from the MS under the influence of alcohol may also lead to meaningful insights.

The suppression of the LFP theta (frequency and power) points towards the fact that some network-level changes take place following acute alcohol administration. The LFP theta is borne out of the interaction of extracellular currents from multiple sources such as the synaptic activity, fast action potentials, calcium spikes, intrinsic currents and resonances, spike afterhyperpolarization, gap junctions and neuron-glia interactions and ephaptic effects (*26*). Thus, it is hard to pinpoint the effect of alcohol seen on the LFP theta to be arising solely out of the firing properties of pyramidal neurons and interneurons. Further, it has been shown in a previous study that it is indeed possible to pace the hippocampal LFP theta via optogenetic stimulation of PV+ cells in the MS (*53*). However, in the present study, it is doubtful if the optogenetic stimulation of the PV+ cells in the medial septum could bring back the theta frequency and power (even though it was seen in some sessions as discussed above). Further, all the mice involved in the septum stimulation trial analysis had proper virus expression and the optic fibre was also implanted at the correct location in the MS. A more comprehensive analysis looking at the effects of optogenetic stimulation on a session by session basis would be performed to evaluate the LFP theta pacing efficiency. Finally, if the septum activation indeed brings back the LFP theta, a pertinent experiment would be to determine if the performance of drunk mice in a memory task improves upon the optogenetic stimulation of PV+ cells in the septum.

Chapter 5

Future Perspectives and Conclusion

5.1 Future Perspectives

Perhaps the clearest deficit of acute alcohol intoxication was seen in the LFP theta. Therefore, apart from the analyses mentioned in the discussion, the LFP, in particular, will be investigated in greater detail. Specifically, a discrete wavelet transform (DWT) calculation will be performed. DWT is a type of time-frequency analysis which breaks down a discrete wavelet (a wave-like oscillation) signal such as the LFP data into different frequency components and gives a good temporal resolution as well. Therefore, it allows one to probe how the different frequency ranges like delta (1-4 Hz), theta (6-12 Hz), alpha (12-25 Hz), gamma (25-140 Hz) behave over time. It will be insightful to look at the effects of acute alcohol intoxication in these other frequency ranges as well. For instance, gamma waves contribute to memory formation and are thought to play a critical role in information processing in the brain (*26*, *98*).

On performing DWT, wavelet coefficients corresponding to different frequency ranges are obtained. Using these coefficients, wavelet entropy (WE), relative wavelet entropy (RWE) and relative wavelet energy will also be calculated. The WE carries information about the degree of order/disorder associated with a multi-frequency signal response (*99*, *100*). It was reported that WE increased upon acute alcohol intoxication (*82*). It will be interesting to compute WE and compare results found in the present study with the previous literature. The RWE compares the similarity between different frequency bands of the signal. The relative wavelet energy, as the name suggests, computes the relative energy associated with each of the frequency bands and thus provides information about their corresponding degree

of importance. Thus, performing the DWT analysis will allow us to gauge the interplay of these various frequency bands which can eventually help us to build top-down models about possible changes in the network following acute alcohol administration.

5.2 Conclusion

This study looked at the effects of acute alcohol intoxication in the CA1 region of the hippocampus in awake, freely behaving PV-cre mice. The study also assessed whether by stimulating the PV+ cells in the MS after alcohol administration, the effects of alcohol on spatial memory could be reversed. It was observed that the mean firing rate and the information score of place cells, along with the location of the place fields remained intact even after acute alcohol administration. However, the mean firing rate of non-spatial cells decreased immediately after injecting alcohol and the mean firing rate of the interneurons also showed a decreasing trend. Further, the LFP theta frequency and power also dropped after acute alcohol administration. Thus, the results of this study provide evidence that acute alcohol intoxication indeed causes changes in both the cellular as well as the network level in the CA1 region of the hippocampus. However, there is a lack of clarity regarding the effect of optogenetic stimulation of the PV+ cells in the MS on the LFP theta after alcohol administration. This study is the first of its kind raising interesting possibilities that need to be tested by additional experiments, which include further electrophysiological recordings and analysis, along with additional fine-tuning of the behavioural paradigms in mice. These experiments can provide important insights into the mechanisms underlying deficits of spatial memory caused by alcohol intoxication and throw further light on the mechanisms of LFP theta pacing by rhythmic activation of the PV+ cells in the MS following alcohol administration.

Bibliography

(*1*) Stock, J. B., and Zhang, S., (2013). The biochemistry of memory. *Current Biology 23*, R741–R745.

(*2*) Ildefonso, M., Bringas, C., Malaina, I., Fedetz, M., Carrasco-Pujante, J., Morales, M., Knafo, S., Martnez, L., Pérez-Samartn, A., López, J. I., et al. (2019). Evidence of conditioned behavior in amoebae. *Nature communications 10*, 1–12.

(*3*) Baddeley, A. D., *Human memory: Theory and practice*; Psychology Press: 1997.

(*4*) Pavlov, I. P., (1960). Conditioned reflex: An investigation of the physiological activity of the cerebral cortex.

(*5*) Squire, L. R., (2004). Memory systems of the brain: a brief history and current perspective. *Neurobiology of learning and memory 82*, 171–177.

(*6*) Tulving, E., (2002). Chronesthesia: Conscious awareness of subjective time.

(*7*) Templer, V. L., and Hampton, R. R., (2013). Episodic memory in nonhuman animals. *Current Biology 23*, R801–R806.

(*8*) Clayton, N. S., Bussey, T. J., and Dickinson, A., (2003). Can animals recall the past and plan for the future? *Nature Reviews Neuroscience 4*, 685–691.

(*9*) Clayton, N. S., Yu, K. S., and Dickinson, A., (2003). Interacting Cache memories: evidence for flexible memory use by Western Scrub-Jays (Aphelocoma californica). *Journal of Experimental Psychology: Animal Behavior Processes 29*, 14.

(*10*) Bracis, C., Gurarie, E., and Bram Van Moorter, R., (2015). Memory effects on movement behavior in animal foraging. *PloS one 10*.

(*11*) Aoki, Y., Igata, H., Ikegaya, Y., and Sasaki, T., (2019). The integration of goal-directed signals onto spatial maps of hippocampal place cells. *Cell reports 27*, 1516–1527.

(*12*) Grieves, R. M., Jenkins, B. W., Harland, B. C., Wood, E. R., and Dudchenko, P. A., (2016). Place field repetition and spatial learning in a multicompartment environment. *Hippocampus 26*, 118–134.

(*13*) Milner, B., (1972). Disorders of learning and memory after temporal lobe lesions in man. *Neurosurgery 19*, 421–446.

(*14*) Scoville, W. B., and Milner, B., (1957). Loss of recent memory after bilateral hippocampal lesions. *Journal of neurology, neurosurgery, and psychiatry 20*, 11.

(*15*) Unal, G., Joshi, A., Viney, T. J., Kis, V., and Somogyi, P., (2015). Synaptic targets of medial septal projections in the hippocampus and extrahippocampal cortices of the mouse. *Journal of Neuroscience 35*, 15812–15826.

(*16*) Van Strien, N., Cappaert, N., and Witter, M., (2009). The anatomy of memory: an interactive overview of the parahippocampal–hippocampal network. *Nature reviews neuroscience 10*, 272–282.

(*17*) Strange, B. A., Witter, M. P., Lein, E. S., and Moser, E. I., (2014). Functional organization of the hippocampal longitudinal axis. *Nature Reviews Neuroscience 15*, 655–669.

(*18*) Ding, S.-L., (2013). Comparative anatomy of the prosubiculum, subiculum, presubiculum, postsubiculum, and parasubiculum in human, monkey, and rodent. *Journal of Comparative Neurology 521*, 4145–4162.

(*19*) Witter, M. P., Groenewegen, H., Da Silva, F. L., and Lohman, A., (1989). Functional organization of the extrinsic and intrinsic circuitry of the parahippocampal region. *Progress in neurobiology 33*, 161–253.

(*20*) Burwell, R. D., (2000). The parahippocampal region: corticocortical connectivity. *Annals-New York Academy of Sciences 911*, 25–42.

(*21*) Eichenbaum, H., Yonelinas, A. P., and Ranganath, C., (2007). The medial temporal lobe and recognition memory. *Annu. Rev. Neurosci. 30*, 123–152.

(*22*) Jacobs, N. S., Allen, T. A., Nguyen, N., and Fortin, N. J., (2013). Critical role of the hippocampus in memory for elapsed time. *Journal of Neuroscience 33*, 13888–13893.

(*23*) Freund, T. F., and Antal, M., (1988). GABA-containing neurons in the septum control inhibitory interneurons in the hippocampus. *Nature 336*, 170–173.

(*24*) Buzsáki, G., and Moser, E. I., (2013). Memory, navigation and theta rhythm in the hippocampal-entorhinal system. *Nature neuroscience 16*, 130.

(*25*) Evans, T., Bicanski, A., Bush, D., and Burgess, N., (2016). How environment and self-motion combine in neural representations of space. *The Journal of physiology 594*, 6535–6546.

(*26*) Buzsáki, G., Anastassiou, C. A., and Koch, C., (2012). The origin of extracellular fields and currentsEEG, ECoG, LFP and spikes. *Nature reviews neuroscience 13*, 407–420.

(*27*) O'Keefe, J., and Dostrovsky, J., (1971). The hippocampus as a spatial map: preliminary evidence from unit activity in the freely-moving rat. *Brain research*.

(*28*) Hafting, T., Fyhn, M., Molden, S., Moser, M.-B., and Moser, E. I., (2005). Microstructure of a spatial map in the entorhinal cortex. *Nature 436*, 801–806.

(*29*) Sargolini, F., Fyhn, M., Hafting, T., McNaughton, B. L., Witter, M. P., Moser, M.-B., and Moser, E. I., (2006). Conjunctive representation of position, direction, and velocity in entorhinal cortex. *Science 312*, 758–762.

(*30*) Solstad, T., Boccara, C. N., Kropff, E., Moser, M.-B., and Moser, E. I., (2008). Representation of geometric borders in the entorhinal cortex. *Science 322*, 1865–1868.

(*31*) Ranck Jr, J., In *Society of Neuroscience Abstract*, 1984; Vol. 10, p 599.

(*32*) Chen, L. L., Lin, L.-H., Green, E. J., Barnes, C. A., and McNaughton, B. L., (1994). Head-direction cells in the rat posterior cortex. *Experimental brain research 101*, 8–23.

(*33*) Taube, J. S., (1995). Head direction cells recorded in the anterior thalamic nuclei of freely moving rats. *Journal of Neuroscience 15*, 70–86.

(*34*) O'Keefe, J., and Burgess, N., (1996). Geometric determinants of the place fields of hippocampal neurons. *Nature 381*, 425–428.

(*35*) Lever, C., Burton, S., Jeewajee, A., O'Keefe, J., and Burgess, N., (2009). Boundary vector cells in the subiculum of the hippocampal formation. *Journal of Neuroscience 29*, 9771–9777.

(*36*) Muller, R. U., and Kubie, J. L., (1987). The effects of changes in the environment on the spatial firing of hippocampal complex-spike cells. *Journal of Neuroscience 7*, 1951–1968.

(*37*) Moser, E. I., Kropff, E., and Moser, M.-B., (2008). Place cells, grid cells, and the brain's spatial representation system. *Annu. Rev. Neurosci. 31*, 69–89.

(*38*) O'Keefe, J., and Recce, M. L., (July 1993). Phase relationship between hippocampal place units and the EEG theta rhythm. *Hippocampus 3*, 317–330.

(*39*) Skaggs, W. E., McNaughton, B. L., Wilson, M. A., and Barnes, C. A., (1996). Theta phase precession in hippocampal neuronal populations and the compression of temporal sequences. *Hippocampus 6*, 149–172.

(*40*) Jaramillo, J., and Kempter, R., (2017). Phase precession: a neural code underlying episodic memory? *Current opinion in neurobiology 43*, 130–138.

(*41*) Stewart, M., and Fox, S. E., (1990). Do septal neurons pace the hippocampal theta rhythm? *Trends in neurosciences 13*, 163–169.

(*42*) Sotty, F., Danik, M., Manseau, F., Laplante, F., Quirion, R., and Williams, S., (2003). Distinct electrophysiological properties of glutamatergic, cholinergic and GABAergic rat septohippocampal neurons: novel implications for hippocampal rhythmicity. *The Journal of physiology 551*, 927–943.

(*43*) Somogyi, P., Tam?s, G., Lujan, R., and Buhl, E. H., (May 1998). Salient features of synaptic organisation in the cerebral cortex. *Brain Res. Brain Res. Rev. 26*, 113–135.

(*44*) Hangya, B., Borhegyi, Z., Szilágyi, N., Freund, T. F., and Varga, V., (2009). GABAergic neurons of the medial septum lead the hippocampal network during theta activity. *Journal of Neuroscience 29*, 8094–8102.

(*45*) Freund, T. F., (1989). GABAergic septohippocampal neurons contain parvalbumin. *Brain research 478*, 375–381.

(*46*) Mamad, O., McNamara, H. M., Reilly, R. B., and Tsanov, M., (2015). Medial septum regulates the hippocampal spatial representation. *Frontiers in behavioral neuroscience 9*, 166.

(*47*) Bolding, K. A., Ferbinteanu, J., Fox, S. E., and Muller, R. U., (2020). Place cell firing cannot support navigation without intact septal circuits. *Hippocampus 30*, 175–191.

(*48*) Ju, W., Santos, A., Freeman, A., Daniele, E., et al. (2018). Neuroscience: Canadian 1st Edition.

(*49*) Boyden, E. S., Zhang, F., Bamberg, E., Nagel, G., and Deisseroth, K., (2005). Millisecond-timescale, genetically targeted optical control of neural activity. *Nature neuroscience 8*, 1263–1268.

(*50*) Hippenmeyer, S., Vrieseling, E., Sigrist, M., Portmann, T., Laengle, C., Ladle, D. R., and Arber, S., (2005). A developmental switch in the response of DRG neurons to ETS transcription factor signaling. *PLoS biol 3*, e159.

(*51*) Cardin, J. A., Carlén, M., Meletis, K., Knoblich, U., Zhang, F., Deisseroth, K., Tsai, L.-H., and Moore, C. I., (2009). Driving fast-spiking cells induces gamma rhythm and controls sensory responses. *Nature 459*, 663–667.

(*52*) Shu, X., Shaner, N. C., Yarbrough, C. A., Tsien, R. Y., and Remington, S. J., (2006). Novel chromophores and buried charges control color in mFruits. *Biochemistry 45*, 9639–9647.

(*53*) Zutshi, I., Brandon, M. P., Fu, M. L., Donegan, M. L., Leutgeb, J. K., and Leutgeb, S., (2018). Hippocampal neural circuits respond to optogenetic pacing of theta frequencies by generating accelerated oscillation frequencies. *Current Biology 28*, 1179–1188.

(*54*) Robbins, T., Ersche, K., and Everitt, B., (2008). Drug addiction and the memory systems of the brain.

(*55*) Sjulson, L., Peyrache, A., Cumpelik, A., Cassataro, D., and Buzsáki, G., (2018). Cocaine place conditioning strengthens location-specific hippocampal coupling to the nucleus accumbens. *Neuron 98*, 926–934.

(*56*) Kutlu, M. G., and Gould, T. J., (Oct. 2016). Effects of drugs of abuse on hippocampal plasticity and hippocampus-dependent learning and memory: contributions to development and maintenance of addiction. *Learn. Mem. 23*, 515–533.

(*57*) Peacock, A., et al. (Oct. 2018). Global statistics on alcohol, tobacco and illicit drug use: 2017 status report. *Addiction 113*, 1905–1926.

(*58*) Fairbairn, C. E., Sayette, M. A., Wright, A. G., Levine, J. M., Cohn, J. F., and Creswell, K. G., (Aug. 2015). Extraversion and the Rewarding Effects of Alcohol in a Social Context. *J Abnorm Psychol 124*, 660–673.

(*59*) Koob, G. F., (2013). Theoretical frameworks and mechanistic aspects of alcohol addiction: alcohol addiction as a reward deficit disorder. *Curr Top Behav Neurosci 13*, 3–30.

(*60*) Gilman, J. M., Ramchandani, V. A., Davis, M. B., Bjork, J. M., and Hommer, D. W., (Apr. 2008). Why we like to drink: a functional magnetic resonance imaging study of the rewarding and anxiolytic effects of alcohol. *J. Neurosci. 28*, 4583–4591.

(*61*) Arts, N. J., Walvoort, S. J., and Kessels, R. P., (2017). Korsakoff's syndrome: a critical review. *Neuropsychiatr Dis Treat 13*, 2875–2890.

(*62*) Miller, M. B., Merrill, J. E., DiBello, A. M., and Carey, K. B., (Oct. 2018). Distinctions in Alcohol-Induced Memory Impairment: A Mixed Methods Study of En Bloc Versus Fragmentary Blackouts. *Alcohol. Clin. Exp. Res. 42*, 2000–2010.

(*63*) White, A. M., (2003). What happened? Alcohol, memory blackouts, and the brain. *Alcohol Res Health 27*, 186–196.

(*64*) Lobo, I. A., and Harris, R. A., (July 2008). GABA(A) receptors and alcohol. *Pharmacol. Biochem. Behav. 90*, 90–94.

(*65*) Olsen, R. W., (Oct. 2014). Analysis of Îş-aminobutyric acid (GABA) type A receptor subtypes using isosteric and allosteric ligands. *Neurochem. Res. 39*, 1924–1941.

(*66*) M?ndez, M., and Morales-Mulia, M., (June 2008). Role of mu and delta opioid receptors in alcohol drinking behaviour. *Curr Drug Abuse Rev 1*, 239–252.

(*67*) Maier, D. M., and Pohorecky, L. A., (Oct. 1986). The effect of ethanol and sex on radial arm maze performance in rats. *Pharmacol. Biochem. Behav. 25*, 703–709.

(*68*) Sircar, R., Basak, A. K., and Sircar, D., (Sept. 2009). Repeated ethanol exposure affects the acquisition of spatial memory in adolescent female rats. *Behav. Brain Res. 202*, 225–231.

(*69*) Acheson, S. K., Bearison, C., Risher, M. L., Abdelwahab, S. H., Wilson, W. A., and Swartzwelder, H. S., (2013). Effects of acute or chronic ethanol exposure during adolescence on behavioral inhibition and efficiency in a modified water maze task. *PLoS ONE 8*, e77768.

(*70*) Steffensen, S. C., and Henriksen, S. J., (Apr. 1992). Comparison of the effects of ethanol and chlordiazepoxide on electrophysiological activity in the fascia dentata and hippocampus regio superior. *Hippocampus 2*, 201–211.

(*71*) Matthews, D. B., Simson, P. E., and Best, P. J., (Apr. 1996). Ethanol alters spatial processing of hippocampal place cells: a mechanism for impaired navigation when intoxicated. *Alcohol. Clin. Exp. Res. 20*, 404–407.

(*72*) White, A. M., and Best, P. J., (Sept. 2000). Effects of ethanol on hippocampal place-cell and interneuron activity. *Brain Res. 876*, 154–165.

(*73*) Ehlers, C. L., Kaneko, W. M., Wall, T. L., and Chaplin, R. I., (Apr. 1992). Effects of dizocilpine (MK-801) and ethanol on the EEG and event-related potentials (ERPS) in rats. *Neuropharmacology 31*, 369–378.

(*74*) Givens, B., (June 1995). Low doses of ethanol impair spatial working memory and reduce hippocampal theta activity. *Alcohol. Clin. Exp. Res. 19*, 763–767.

(*75*) Givens, B., Williams, J. M., and Gill, T. M., (2000). Septohippocampal pathway as a site for the memory-impairing effects of ethanol. *Hippocampus 10*, 111–121.

(*76*) Harrison, N. L., Skelly, M. J., Grosserode, E. K., Lowes, D. C., Zeric, T., Phister, S., and Salling, M. C., (Aug. 2017). Effects of acute alcohol on excitability in the CNS. *Neuropharmacology 122*, 36–45.

(*77*) Maier, D. M., and Pohorecky, L. A., (1986). The effect of ethanol and sex on radial arm maze performance in rats. *Pharmacology Biochemistry and Behavior 25*, 703–709.

(*78*) Gil, M., Ancau, M., Schlesiger, M. I., Neitz, A., Allen, K., De Marco, R. J., and Monyer, H., (2018). Impaired path integration in mice with disrupted grid cell firing. *Nature neuroscience 21*, 81–91.

(*79*) Bokil, H. S., Andrews, P., Maniar, H., Pesaran, B., Kulkarni, J., Loader, C., and Mitra, P. P., (2009). Chronux: a platform for analyzing neural signals. *BMC Neuroscience 10*, S3.

(*80*) Lee, H., Roh, S., Kim, D. J., et al. (2009). Alcohol-induced blackout. *International journal of environmental research and public health 6*, 2783–2792.

(*81*) Ludvig, N., Altura, B. T., Fox, S. E., and Altura, B. M., (1995). The suppressant effect of ethanol, delivered via intrahippocampal microdialysis, on the firing of local pyramidal cells in freely behaving rats. *Alcohol 12*, 417–421.

(*82*) Zhang, Y., Yu, H., Li, W., Yang, Y., Wang, X., and Qian, Z., (2016). Effect of acute ethanol administration on the hippocampal region neural activity using a microelectrode array. *Alcoholism: Clinical and Experimental Research 40*, 1857–1864.

(*83*) Little, H., (1991). Mechanisms that may underlie the behavioural effects of ethanol. *Progress in neurobiology 36*, 171–194.

(*84*) Siggins, G., Bloom, F., French, E. D., Madamba, S., Mancillas, J., Pittman, Q., and Rogers, J., (1987). Electrophysiology of ethanol on central neurons. *Annals of the New York Academy of Sciences 492*, 350–366.

(*85*) Lyons, D., Miller, M. D., Hedgecock-Rowe, A. A., Crane, A. M., and Porrino, L. J., (1998). Time-dependent effects of acute ethanol administration on regional cerebral blood flow in the rat. *Alcohol 16*, 213–219.

(*86*) Livy, D. J., Parnell, S. E., and West, J. R., (2003). Blood ethanol concentration profiles: a comparison between rats and mice. *Alcohol 29*, 165–171.

(*87*) Hyman, J. M., Wyble, B. P., Goyal, V., Rossi, C. A., and Hasselmo, M. E., (2003). Stimulation in hippocampal region CA1 in behaving rats yields long-term potentiation when delivered to the peak of theta and long-term depression when delivered to the trough. *Journal of Neuroscience 23*, 11725–11731.

(*88*) Bouwman, B., Van Lier, H., Nitert, H., Drinkenburg, W., Coenen, A., and Van Rijn, C., (2005). The relationship between hippocampal EEG theta activity and locomotor behaviour in freely moving rats: effects of vigabatrin. *Brain research bulletin 64*, 505–509.

(*89*) Bland, B., and Vanderwolf, C., (1972). Electrical stimulation of the hippocampal formation: Behavioral and bioelectrical effects. *Brain Research 43*, 89–106.

(*90*) Bland, B. H., and Oddie, S. D., (2001). Theta band oscillation and synchrony in the hippocampal formation and associated structures: the case for its role in sensorimotor integration. *Behavioural brain research 127*, 119–136.

(*91*) Li, J.-Y., Kuo, T., Hsieh, I.-T., and Yang, C., (2012). Changes in hippocampal theta rhythm and their correlations with speed during different phases of voluntary wheel running in rats. *Neuroscience 213*, 54–61.

(*92*) Shin, J., and Talnov, A., (2001). A single trial analysis of hippocampal theta frequency during nonsteady wheel running in rats. *Brain research 897*, 217–221.

(*93*) Sinnamon, H., (2006). Decline in hippocampal theta activity during cessation of locomotor approach sequences: amplitude leads frequency and relates to instrumental behavior. *Neuroscience 140*, 779–790.

(*94*) Vanderwolf, C. H., (1969). Hippocampal electrical activity and voluntary movement in the rat. *Electroencephalography and clinical neurophysiology 26*, 407–418.

(*95*) Oddie, S. D., and Bland, B. H., (1998). Hippocampal formation theta activity and movement selection. *Neuroscience & Biobehavioral Reviews 22*, 221–231.

(*96*) Ognjanovski, N., Schaeffer, S., Wu, J., Mofakham, S., Maruyama, D., Zochowski, M., and Aton, S. J., (2017). Parvalbumin-expressing interneurons coordinate hippocampal network dynamics required for memory consolidation. *Nature communications 8*, 1–14.

(*97*) Rowland, D. C., Roudi, Y., Moser, M.-B., and Moser, E. I., (2016). Ten years of grid cells. *Annual review of neuroscience 39*, 19–40.

(*98*) Bartos, M., Vida, I., and Jonas, P., (2007). Synaptic mechanisms of synchronized gamma oscillations in inhibitory interneuron networks. *Nature reviews neuroscience 8*, 45–56.

(*99*) Rosso, O. A., Blanco, S., Yordanova, J., Kolev, V., Figliola, A., Schürmann, M., and Baar, E., (2001). Wavelet entropy: a new tool for analysis of short duration brain electrical signals. *Journal of neuroscience methods 105*, 65–75.

(*100*) Kumar, Y., Dewal, M., and Anand, R., In *2013 IEEE international conference on signal processing, computing and control (ISPCC)*, 2013, pp 1–6.